



**Politecnico  
di Torino**



**Politecnico di Torino**

Master of Science Program in Energy and Nuclear Engineering  
Academic year 2023/2024  
March 2024

# **Organic fraction of municipal solid waste treatment plant optimization case study**

Circular economy sustainable transition toward high efficiency Solid Oxide  
Fuel Cell stack system

Supervisor:

Prof. Massimo Santarelli

Candidate:

Marco Maio



ad Antonio

*"You may not be responsible for the situation you are in, but you will become responsible if you do nothing to change it."*

*“Può darsi che non siate responsabili per la situazione in cui vi trovate, ma lo diventerete se non fate nulla per cambiarla.”*

Martin Luther King

# ABSTRACT

The purpose of this study aims to be the energy optimization of a A2A Energiefuture project for an organic fraction of municipal solid waste treatment plant located in San Filippo del Mela. The plant is designed to dispose of an amount of about 75'000 tons per year of organic waste. By means of an anaerobic digestion process, and thus in the absence of oxygen, the fermentation of the organic fraction generates biogas and compost. The former, main focus of this study, once treated and filtered to remove impurities, can be injected, in accordance with the ongoing incentives, into the national gas distribution network as biomethane since it is characterized by similar parameters. The plant's energy demands, both thermal and electrical, are satisfied through withdrawal from the grid in the base configuration. Thermal energy required to maintain the operating temperature of the digester and to preheat the air for the biocells is provided by two similar boilers of 780 kW each fired by natural gas. Electricity supply is provided by a MV electrical substation. An optimized solution has been analysed in which natural gas-fired boilers give way to fuel cell also fed by natural gas. The latter electrochemical device can not only cover both the thermal and electrical needs of the plant but can also generate an electricity surplus that can be injected into the grid or stored in a battery energy system. Moreover a "stand-alone island" configuration was also analysed in which the fuel cell stack is fed by a share of biomethane produced by the treatment plant. The latest configuration, beyond reducing net carbon dioxide emissions to almost zero, provides the significant opportunity to not depend on natural gas market price fluctuations. A model has been created on Aspen Plus® that breaks down the electrochemical process through all the reactions that occur within each fuel cell component. By means of the model, it was possible to run the simulation by which the operating values of the fuel cell under the steady-state conditions were obtained. These parameters were extracted and used in a calculator data sheet to achieve the economic analysis of the new plant design.

# CONTENTS

|   |    |
|---|----|
| <b>List of figures</b> .....  | 7  |
| <b>List of tables</b> .....   | 9  |
| 1. Introduction.....  | 11 |
| 1.2 Global overview.....  | 11 |
| 1.3 Applied circular economy: Waste to Energy (WTE) .....                       | 16 |
| 2. Technologies .....   | 19 |
| 2.1 Fuel Cell .....   | 19 |
| 2.1.1 Solid Oxide Fuel Cell .....   | 23 |
| 2.2 Organic fraction of municipal solid waste treatment and recovery plant..... | 30 |
| 2.2.1 Anaerobic digestion process .....   | 33 |
| 2.2.2 Composting process.....   | 35 |
| 2.3 SOFC & OFMSW.....   | 35 |
| 3. ASPEN Model.....   | 37 |
| 3.1 SOFC layout.....  | 37 |
| 3.2 SOFC Anode .....  | 38 |
| 3.3 SOFC Cathode .....  | 41 |
| 3.4 SOFC heat recovery and pre-heating system.....                              | 41 |
| 4. Results .....  | 44 |
| 4.1 Standard configuration.....   | 44 |
| 4.2 Natural gas fed SOFC stack configuration.....                               | 46 |
| 4.3 Island SOFC configuration .....   | 50 |
| 4.4 Considerations.....   | 53 |
| <b>REFERENCES</b> .....   | 57 |

# List of figures

|  |    |
|--|----|
| <b>Figure 1.1</b> – Net global greenhouse gas emissions [1] .....  | 11 |
| <b>Figure 1.2</b> - Global greenhouse gas emissions by sector. The above picture is referred to 2016, during which the total amount of greenhouse emissions were 49.4 billion tons CO <sub>2</sub> eq [2]..... | 12 |
| <b>Figure 1.3</b> - Observed (1900–2020) and projected (2021–2100) changes in global surface temperature (relative to 1850–1900) [1].....  | 13 |
| <b>Figure 1.4</b> – Gross inland consumption of energy [3] .....   | 16 |
| <b>Figure 1.5</b> - Linear vs Circular economy .....   | 17 |
| <b>Figure 1.6</b> - Waste cycle processed by anaerobic digestion .....   | 18 |
| <b>Figure 2.1</b> - Functioning scheme of the fuel cell .....  | 19 |
| <b>Figure 2.2</b> - Energy transformation comparison.....  | 21 |
| <b>Figure 2.3</b> - Fuel cell classification .....   | 22 |
| <b>Figure 2.4</b> - Ohmic resistance for R1 and YSZ as a function of temperature [6] .....   | 25 |
| <b>Figure 2.5</b> - Perovskite structure .....   | 26 |
| <b>Figure 2.6</b> - PEMFC and SOFC performance comparison [7].....   | 27 |
| <b>Figure 2.7</b> - Carbon whisker [8] .....   | 27 |
| <b>Figure 2.8</b> - Carbon deposition limit boundaries for a C-H-O composition for various types of hydrocarbons [9].....  | 28 |
| <b>Figure 2.9</b> - OFSMW treatment process scheme.....  | 30 |
| <b>Figure 2.10</b> - Steps of the methanogenesis process [10] .....  | 34 |
| <b>Figure 3.1</b> - SOFC ASPEN layout.....   | 37 |
| <b>Figure 3.2</b> - Anode recirculation loop.....  | 39 |

|   |    |
|---|----|
| <b>Figure 3.3</b> - Cathode air heat exchange.....  | 41 |
| <b>Figure 3.4</b> - Fuel cell thermal balance .....   | 42 |
| <b>Figure 3.5</b> - Simulation results.....   | 43 |
| <b>Figure 4.1</b> - Natural gas fed SOFC configuration NPV .....                              | 49 |
| <b>Figure 4.2</b> – Natural gas fed SOFC PBT Fuel cell unitary cost sensitivity analysis..... | 49 |
| <b>Figure 4.3</b> – Natural gas fed SOFC NPV fuel cell unitary cost sensitivity analysis..... | 50 |
| <b>Figure 4.4</b> – Island SOFC configuration NPV .....                                       | 52 |
| <b>Figure 4.5</b> – Island SOFC PBT Fuel cell unitary cost sensitivity analysis .....         | 52 |
| <b>Figure 4.6</b> – Island SOFC NPV fuel cell unitary cost sensitivity.....                   | 53 |



# List of tables

|   |    |
|---|----|
| <b>Table 2.1</b> - Fuel cell properties .....   | 23 |
| <b>Table 2.2</b> - Advantages/Disadvantages anaerobic technologies DRY and WET .....    | 31 |
| <b>Table 2.3</b> - Upgrading technologies Advantages/Disadvantages .....                | 32 |
| <b>Table 3.1</b> - Biomethane parameters .....  | 40 |
| <b>Table 4.1</b> - Electrical consumption breakdown .....                               | 45 |
| <b>Table 4.2</b> - Base case configuration costs breakdown .....                        | 45 |
| <b>Table 4.3</b> – Natural gas parameters.....  | 46 |
| <b>Table 4.4</b> – Natural gas fed SOFC configuration energy consumption and production | 47 |
| <b>Table 4.5</b> - Natural gas fed SOFC configuration costs breakdown .....             | 48 |
| <b>Table 4.6</b> – Biomethane parameters .....  | 50 |
| <b>Table 4.7</b> – Island SOFC configuration energy consumption and production .....    | 51 |
| <b>Table 4.8</b> – Island SOFC configuration costs breakdown .....                      | 51 |
| <b>Table 4.9</b> – Configurations comparison.....                                       | 54 |



# 1. Introduction

Over the past 80 years, humanity has experienced a significant increase in carbon dioxide concentrations in the atmosphere, mostly due to human activities such as fossil fuel burning, industries, and deforestation. The increase in carbon dioxide has contributed to global warming and climate change, with significant impacts on weather, ecosystems, and human health. An analysis of historical carbon dioxide data provides clear evidence of the link between anthropogenic activities and rising greenhouse gas concentrations in the atmosphere. In the context of the current economic and energy scenario, the necessity of developing sustainable and innovative waste management solutions assumes a crucial role. The growing awareness of the human footprint on climate change has made it mandatory to adopt approaches that not only reduce environmental impacts but also help mitigate root causes. In this scenario, the approach to managing the organic fraction of municipal solid waste (OFMSW) presents itself as a breakthrough opportunity.

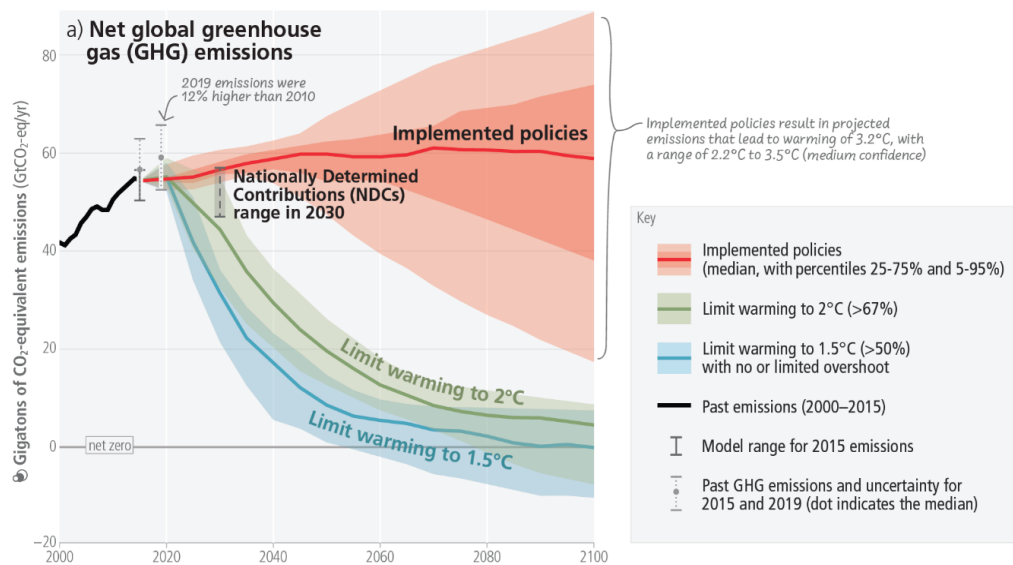


Figure 1.1 – Net global greenhouse gas emissions [1]

## 1.2 Global overview

Climate change is one of the most urgent and pressing challenges facing humanity today. One of its main causes is the increase in the concentration of greenhouse gases, especially carbon dioxide (CO<sub>2</sub>), in the atmosphere. This increase is largely due to human activities, in particular the burning of fossil fuels

and inefficient waste management. CO<sub>2</sub> emissions from human activities Human activities are responsible for a significant amount of CO<sub>2</sub> emissions into the atmosphere. The main contributors can be summarized in:

- Burning of fossil fuels: The use of coal, oil and natural gas for energy production and transport is a major source of CO<sub>2</sub> emissions. Coal-fired power plants are particularly harmful, emitting large amounts of CO<sub>2</sub> during combustion;
- Transport: The use of motor vehicles, both private and commercial, is a major contributor to CO<sub>2</sub> emissions. This includes cars, lorries, planes and ships;
- Industry: Industrial processes such as the production of cement, steel, aluminium and other heavy materials can emit significant amounts of CO<sub>2</sub>;
- Deforestation and land-use change: Deforestation and conversion of forest land to agricultural or urban land results in the loss of forest biomass, which sequesters CO<sub>2</sub>. In addition, intensive agriculture can release CO<sub>2</sub> into the soil.

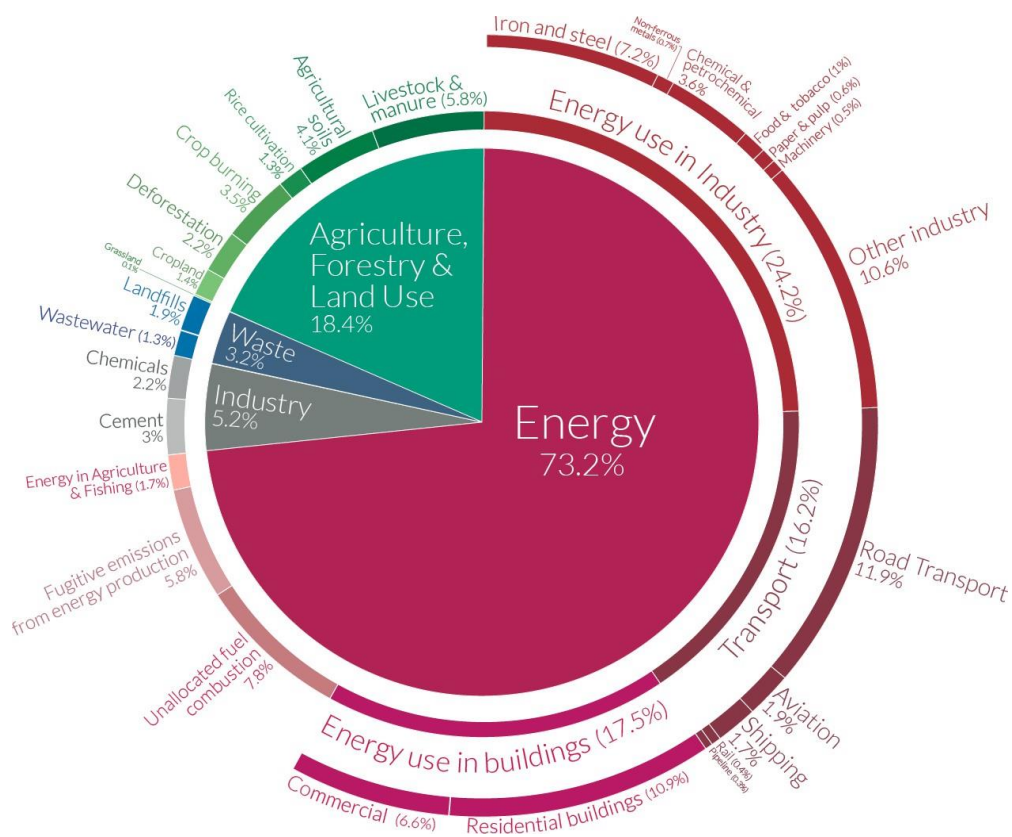


**Figure 1.2** - Global greenhouse gas emissions by sector. The above picture is referred to 2016, during which the total amount of greenhouse emissions were 49.4 billion tons CO<sub>2eq</sub> [2]

The consequences of this increase in carbon dioxide in the atmosphere are mainly environmental and human, through global warming. The most obvious effects are:

- Increased temperatures: Global warming leads to an increase in average global temperatures, resulting in hotter summers, more frequent and longer heat waves, and milder winters.
- Melting glaciers and rising sea levels: Global warming is causing glaciers and polar ice caps to melt, contributing to rising sea levels. This phenomenon threatens coastal communities and fragile ecosystems.
- Extreme weather events: Climate change increases the frequency and intensity of extreme weather events such as storms, hurricanes, torrential rains and droughts, causing damage to infrastructure, agricultural crops and human communities.
- Impacts on ecosystems: Climate change is causing habitat shifts and changes in species distribution patterns, threatening biodiversity and ecosystem services.

The global annual mean temperature approached 1.5°C above pre-industrial levels - a symbolic figure because the Paris Agreement on climate change aims to limit the long-term temperature increase (averaged over decades rather than a single year such as 2023) to no more than 1.5°C above pre-industrial levels.

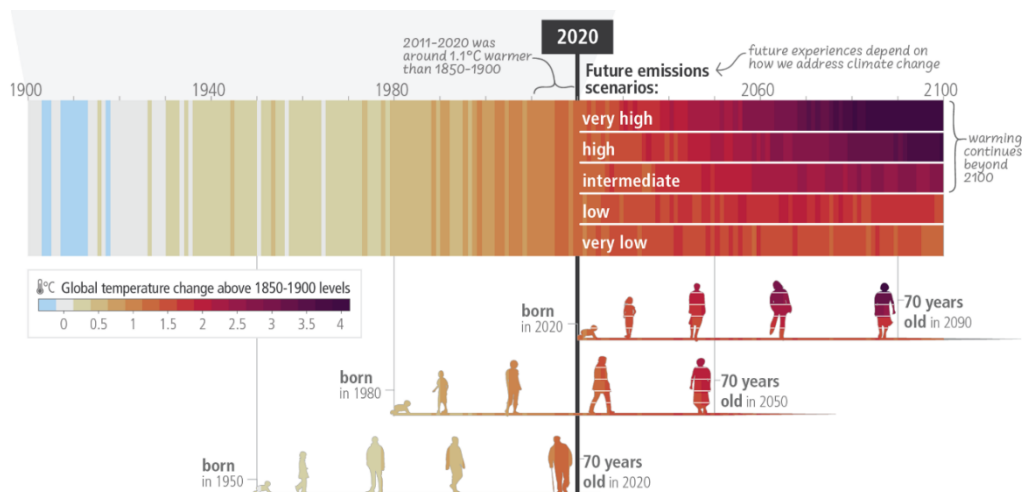


**Figure 1.3** - Observed (1900–2020) and projected (2021–2100) changes in global surface temperature (relative to 1850–1900) [1]

Six of the main international datasets used to monitor global temperatures, consolidated by the WMO, show that the global annual mean temperature in 2023 was  $1.45 \pm 0.12$  °C above pre-industrial (1850-1900) levels. Global temperatures set new monthly records in every month between June and December. July and

August were the two warmest months on record. Long-term monitoring of global temperatures is only one indicator of climate and its change. Other key indicators include atmospheric greenhouse gas concentrations, ocean warming and acidification, sea level, sea ice extent and glacier mass balance. The WMO interim report on the state of the global climate in 2023, published on 30 November, shows that records have been broken across the board. Sea surface temperatures were exceptionally high for much of the year, accompanied by severe and damaging ocean heat waves. Antarctic sea ice extent was the lowest ever recorded, both for the late summer minimum in February and the late winter maximum in September. These long-term climate changes are manifested in daily weather conditions. In 2023, extreme heat took its toll on health and helped fuel devastating wildfires. Heavy rains, floods and rapidly intensifying tropical cyclones have left a trail of destruction, death and huge economic losses. Europe achieved the targets of the 2020 climate package ahead of schedule, but in the new 2030 package it has set targets (27% renewables in gross final consumption and a 30% reduction in trend energy consumption) that are unlikely to meet the 40% greenhouse gas reduction target. Implementing the Paris Agreement will require an improvement in Europe's 2030 targets. Europe is also on the verge of adopting a major new directive on waste and the circular economy, with the ambitious goal of making the European economy the most resource-efficient in the world, and thus both greener and more competitive.

*“As Europeans, we want to leave a healthier planet behind for those that follow. We obviously cannot turn a blind eye to the climate challenge; we must look to the future”.*

**JEAN-CLAUDE JUNKER**

President of the European Commission, State of the Union address, September 2018

*“The European Union has already started the modernisation and transformation towards a climate-neutral economy. The European Commission is stepping up the efforts as we propose a strategy for Europe to become the world’s first major economy to go climate-neutral by 2050. Going climate-neutral is necessary, possible and in Europe’s interest”.*

**MIGUEL ARIAS CAÑETE**

Commissioner for Climate Action and Energy, on the European Commission’s strategic long-term vision for a prosperous, modern, competitive and climate-neutral economy by 2050, presented on 28 November 2018

In November 2018, the European Commission presented a long-term strategic vision to reduce greenhouse gas (GHG) emissions, showing how Europe can lead the way to climate neutrality - an economy with net zero GHG emissions [3]. The strategy explores how this can be achieved by looking at sectors, including energy, transport, industry and agriculture, industry and agriculture. A portfolio of options has been examined to underline that it is possible to move to net zero GHG emissions by 2050. emissions by 2050, based on existing - and in some cases emerging - technological emerging - technological solutions, empowering citizens and empowering citizens and aligning actions in key areas such as industrial policy, finance or research, while ensuring social equity for a just for a just transition. The European Commission's vision outlines seven key [3] strategic building blocks:

- Maximising the benefits of energy efficiency, including zero emission buildings;
- maximising the use of renewable energy and electricity to fully decarbonise Europe's energy supply;
- clean, safe and connected mobility;
- a competitive EU industry and circular economy as a key enabler to reduce greenhouse gas emissions;
- Developing adequate smart grid infrastructure and interconnections;
- reaping the full benefits of the bio-economy and creating significant carbon sinks;
- address remaining CO<sub>2</sub> emissions with Carbon Capture and storage (CCS).

Realising these building blocks, starting with the implementation of the 2030 climate and energy framework, will enable the EU to make progress towards a prosperous, low-carbon economy. The European Commission's strategic vision responds to the Paris Agreement's call for continued efforts to limit global warming to 1.5°C above pre-industrial levels. It is also fully in line with the UN Sustainable Development Goals. The EU is now on track to meet its own climate and energy targets for 2020 and has set the framework to achieve its 2030 targets for further emission reductions and the transition to clean energy. Together, these policies will enable the EU to make its contribution under the Paris Agreement to reduce emissions by at least 40% by 2030 compared to 1990. 2030, compared to 1990. In fact, the new 2030 targets for energy efficiency and renewables, if fully implemented, should enable the EU to reduce emissions by around 45%. Improved energy efficiency can help cut the EU's energy consumption by around half compared to 2005 levels, playing a key role in achieving greenhouse gas emissions by 2050. Significant progress has already been made: EU primary

energy consumption peaked in 2006 and the EU recently agreed a new binding energy efficiency target of 32.5% by 2030. The transition to clean energy should lead to a system in which the majority of the EU's primary energy supply comes from renewable energy sources, improving security of supply and supporting domestic job development, as well as reducing emissions. The EU recently adopted a new renewable energy target of 32% by 2030.

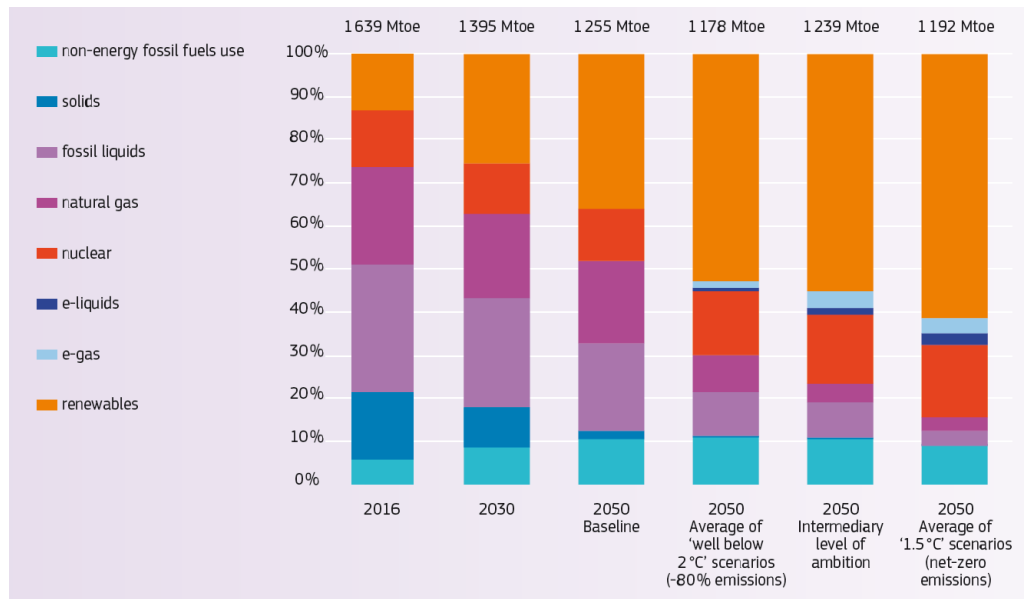


Figure 1.4 – Gross inland consumption of energy [3]

Maintaining a competitive European industry, currently one of the most efficient in the world, goes hand in hand with the efficient use of resources and the development of a circular economy.

### 1.3 Applied circular economy: Waste to Energy (WTE)

*“A circular economy is a regenerative system in which resource input and waste, emission, and energy leakage are minimized by slowing, closing, and narrowing energy and material loops; this can be achieved through long-lasting design, maintenance, repair, reuse, remanufacturing, refurbishing, recycling, and upcycling”.*

## JOURNAL OF CLEANER PRODUCTION

Generating electricity, heat or fuel from what is no longer needed. Waste-to-Energy (WTE) is another aspect of the circular economy that is often less well known than recycling or reuse, and in any case less preferred than the latter.



It is also a controversial aspect that does not fail to generate doubts and uncertainties about its use, as incineration is not among the optimal solutions for achieving an environmentally sustainable waste cycle.

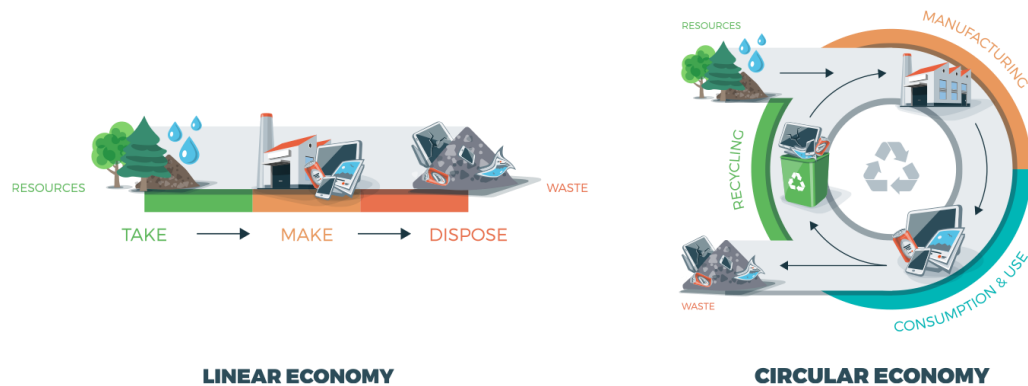


Figure 1.5 - Linear vs Circular economy

In fact, in a hierarchy of preferred waste management actions, energy recovery occupies the penultimate position after waste prevention, preparation for re-use and recycling. The production of energy from waste can continue to play a role in the decarbonisation pathway as a complement to the development of recycling and the management of waste derived from it, and the minimisation of landfill is represented precisely by the recovery of energy from waste. Biomethane is also gaining increasing attention as part of the energy transition to a low-carbon society. The European Union has set ambitious targets to reduce greenhouse gas emissions and promote the use of renewable energy. Biomethane is recognised as a strategic option for decarbonising the natural gas sector. The RePowerEU plan (created to promote the EU's independence from fossil fuels) sets a production target of 35 billion cubic metres of biomethane by 2030, paving the way for investment opportunities in Europe. However, Italy's National Integrated Energy and Climate Plan (PNRR) envisages an increase in biomethane production, with the aim of reaching an installed capacity of 5.5 billion cubic metres by 2030, both through the construction of new plants and the conversion of some of the biogas plants currently in operation to electricity. This represents a significant opportunity for the country's biomethane sector, which the government has encouraged with specific measures in the PNRR. The specific focus of this study is on biomethane produced by anaerobic digestion of the organic fraction of municipal solid waste. This process falls under the previously mentioned themes of circular economy and waste to energy, biomethane production from renewable sources to reduce the emission of carbon dioxide into the atmosphere and energy optimisation of production facilities since the

anaerobic digestion plant is subject to optimisation by Solid Oxide Fuel Cells (SOFC) instead of traditional natural gas-fired boilers.

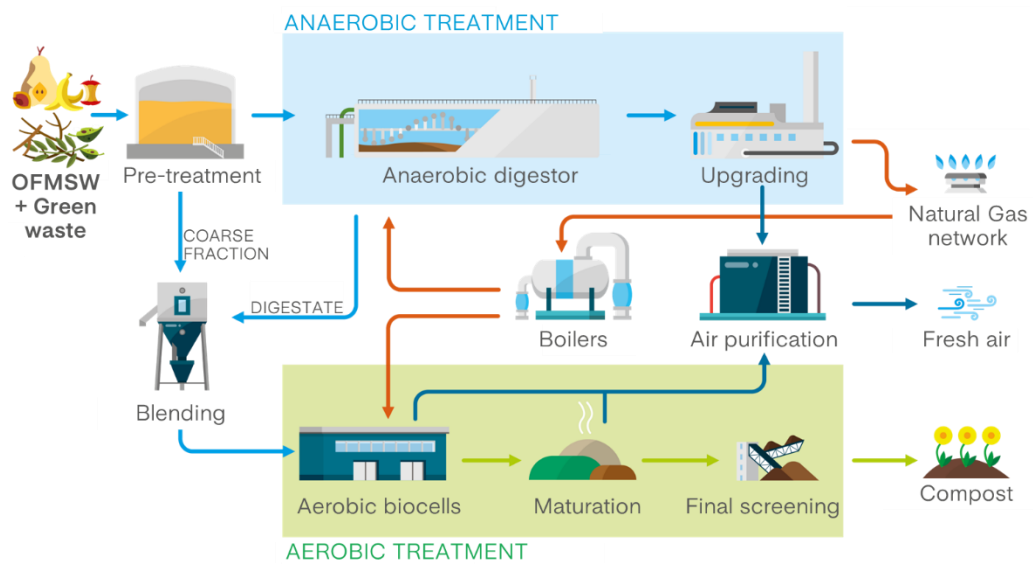


Figure 1.6 - Waste cycle processed by anaerobic digestion

## 2. Technologies

### 2.1 Fuel Cell

Fuel cells (FCs) are electrochemical devices that convert chemical reaction energy directly into electrical energy, without the intermediate intervention of a thermodynamic cycle. The basic structure of a fuel cell consists of an electrolyte in contact with a porous anode and cathode. Figure 2.1 shows a generic cell feed with hydrogen and oxygen gases. The flow directions of involved charges have been indicated, which include both electrons and ions, the latter potentially cations or anions depending on the characteristics of the cell considered.

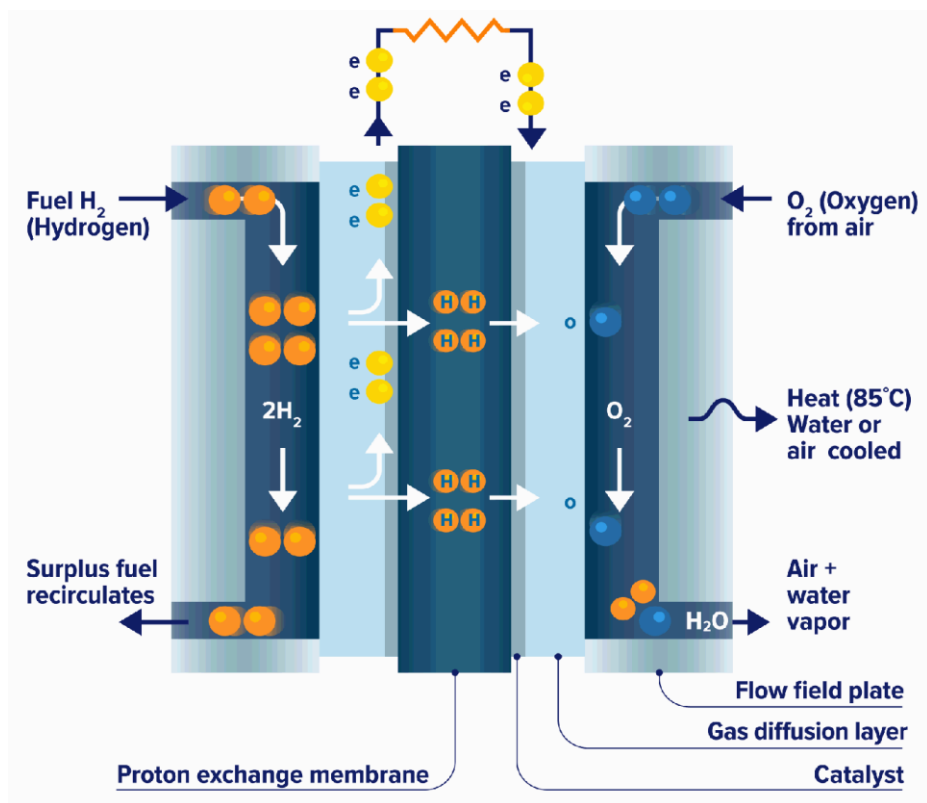


Figure 2.1 - Functioning scheme of the fuel cell

The gaseous fuel feeds the anode while the oxidizing agent, usually oxygen in the air, feeds the cathode continuously; the electrochemical reactions produce directly an electric current at the electrodes. Therefore, it is essential to underline how FCs differ in various aspects from both the classic battery and the rechargeable one; The latter, in fact, can be defined as energy storage devices whose maximum available quantity is determined by that of the stored chemical reagent. The battery ceases to produce electricity when the chemical reagents are consumed. In the refillable version, the reagents are regenerated by the intervention of an external source. The fuel cell, on the other hand, has the

possibility to produce electricity if the electrodes are powered. It should be pointed out, however, that this statement is only valid in theory and that the service life is limited mainly by corrosion and degradation of some of the components. As far as the operating principle is concerned, the fuel and the oxidizing gas penetrate respectively through the anode and the cathode, which are generally positioned on opposite sides of the electrolyte: the electrical energy is generated by the electrochemical oxidation of the fuel and the electrochemical reduction of the oxidant. The redox reactions necessary for cell operation can only occur at ternary interphases, where the gaseous (feed gas) and solid (electrode, electrolyte) phases coexist; these zones are commonly referred to as TPBs, an acronym for Triple Phase Boundaries. The nature and characteristics of these interphases play a critical role in the electrochemical performance of a fuel cell. The operating principle of the electrolyte consists in conducting the ionic charge between the electrodes and then completing the electrical circuit, as illustrated in figure 2.1, and it also constitutes a physical barrier that prevents direct contact between the oxidizer and the fuel. As far as porous electrodes are concerned, they must be able to:

- have accessible active sites where ionization or deionization reactions of gases can take place;
- transport electrons to/from the external circuit through bulk;
- transport the ions from the TPB to the electrolyte.

Therefore, the material for the electrodes must be catalytically active, conductive and porous in order to optimize the efficiency of the reactions. FCs have considerable advantages, first of all a higher efficiency compared to that of common combustion engines, both because it is not limited, as for the latter, by the Carnot cycle, and because of the possibility of exploiting the thermal energy developed and generating additional current through the coupling of a turbine or a steam engine; Cogeneration leads to a conversion efficiency of more than 70% (Figure 2.2). There is also the possibility of reusing part of the heat generated in the fuel pre-treatment phase (reforming); this makes it possible to use different fuels, such as natural gas, pre-treated in a self-sustaining system. A second factor that support the development and optimization of FCs, is the reduced environmental impact directly related to the nature of the exhaust gases, which are basically composed of water vapour, exclusively in the case of hydrogen-fed cells.

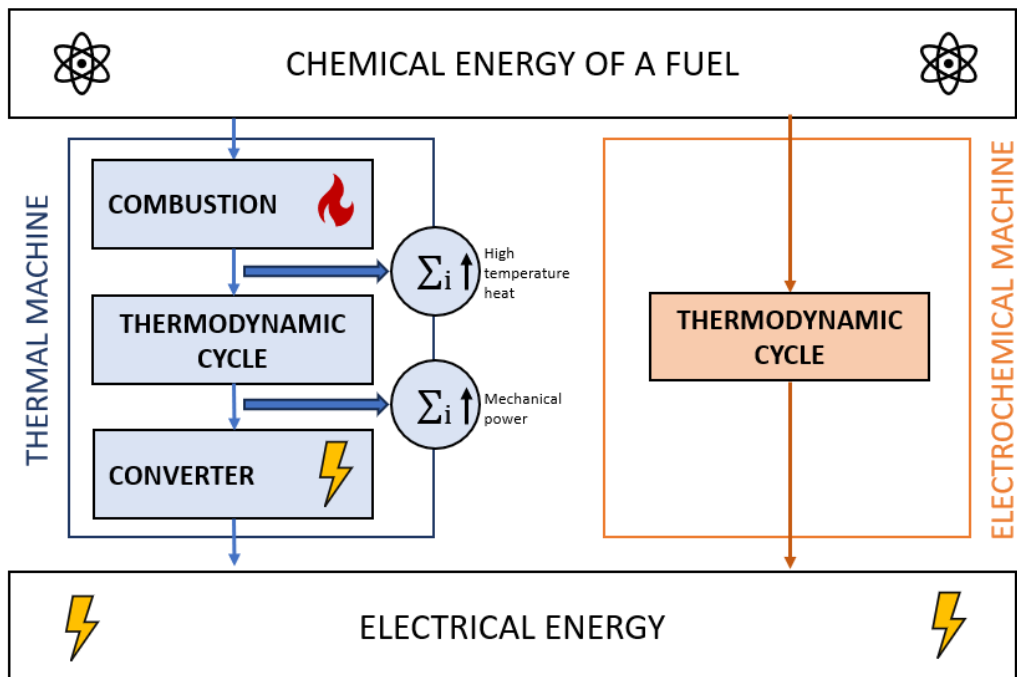


Figure 2.2 - Energy transformation comparison

The first model of FC dates to 1839 and its invention is attributed to the scientist and lawyer William Grove. This consisted of a battery of cells, each consisting of two tubes turned upside down in a solution of sulfuric acid, containing oxygen at the cathode and hydrogen at the anode, respectively, in which two metal wires had been drawn. A cell for the electrolysis of water was connected to the poles of this battery. The recombination of the gases produced was accompanied by a limited flow of electricity. In this first FC, powered by  $H_2$  and  $O_2$ , the half-reactions at the electrodes were respectively:

- Anode:  $H_2 \rightarrow 2H^+ + 2e^-$
- Cathode:  $O_2 + 4e^- \rightarrow 2O_2^-$

and the overall reaction:  $2H_2 + O_2 \rightarrow 2H_2O$ .

The low efficiency in terms of developed current was basically due to three reasons:

- i. the reduced extension of the TPB;
- ii. the high resistance of the ions flow through electrolyte;
- iii. the reduced speed of reactions at the electrodes.

Almost two centuries later, the overall scheme of a fuel cell has remained akin to the original model. Grove's invention remained in the background for about a century, until in the first half of the 20th century such devices began to be looked at with increasing interest. The actual successful applications have taken place in the aerospace field since the 1960s as part of NASA programs [4]. Only towards the end of the twentieth century, under the stimulus of the energy and environmental problems of global interest, previously discussed, the attention to this energy conversion system as a possible alternative/integration to the common devices in use increases. Since the first research conducted in the early 1900s, attempts have been made to solve the basic structural and kinetic problems, which are the causes of the reduced performance found; the different strategies that have been applied so far for improvement purposes have led to the development of different types of FCs that find various industrial applications.

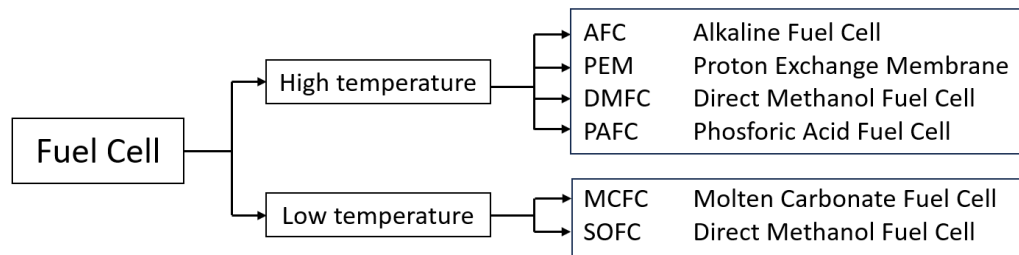


Figure 2.3 - Fuel cell classification

A first distinction can be based on operating temperatures; From this classification, FCs can essentially be divided into High-Temperature Fuel Cells, operating between 500 and 1000 °C, and Low-Temperature Fuel Cells, operating below 500 °C. A further subdivision in the literature has been made based on the nature of the electrolyte and according to this criterion six different types of cells are mainly distinguished. The above figure shows a classification scheme that considers both criteria of distinction (Fig. 2.3).

Consequently, regarding their functioning, the FCs can be classified by:

- for the fuel supply and/or its treatment mode (internal/external reforming);
- for the half-reactions that take part in the two electrodes and consequently for the conduction (type of mobile ion and direction of displacement) to the electrolyte;
- for the type of end-use application to which each class of FCs may be directed.

The main properties and applications are summarized in the table 2.1 [4, 5].

**Table 2.1** - Fuel cell properties

|  | <b>AFC</b>                                     | <b>PEMF</b>                   | <b>DMFC</b>                            | <b>PAFC</b>  | <b>MCFC</b>                            | <b>SOFC</b>                  |
|--|--|-------------------------------|--|--|--|------------------------------|
| <b>Operating Temperature (°C)</b>        | < 100  | 60 - 120                      | 60 - 120                               | 160 - 220  | 600 - 800                              | 800 – 1000<br>500 - 600      |
| <b>Anode Reaction</b>                    | $H_2 + 2OH^- = 2H_2O + 2e^-$                   | $H_2 = 2H^+ + 2e^-$           | $CH_3OH + H_2O = CH_3^+ + 6H^+ + 6e^-$ | $H_2 = 2H^+ + 2e^-$  | $H_2 + CO_3^{2-} = H_2O + CO_2 + 2e^-$ | $H_2 + O^{2-} = H_2O + 2e^-$ |
| <b>Cathode reaction</b>                  | $1/2O_2 + H_2O + 2e^- = 2OH^-$                 | $1/2O_2 + 2H^+ + 2e^- = H_2O$ | $3/2O_2 + 6H^+ + 6e^- = 3H_2O$         | $1/2O_2 + 2H^+ + 2e^- = H_2O$  | $1/2O_2 + 2e^- = CO_3^{2-}$            | $1/2O_2 + 2e^- = O^{2-}$     |
| <b>Applications</b>                      | Transportation Sector<br>Aerospace<br>Military |                               |  | Decentralized stationary systems<br>Transport sector<br>Combined systems: heat and electricity |  |                              |
| <b>Power Achieved</b>                    | 5 -150 kW                                      | 5 -250 kW                     | 5 kW                                   | max 10 MW  | max 2 MW                               | max 250 kW                   |
| <b>Charge carrier in the electrolyte</b> | $OH^-$   | $H^+$                         | $H^+$                                  | $H^+$  | $CO_3^{2-}$                            | $O^{2-}$                     |

### 2.1.1 Solid Oxide Fuel Cell

In high temperature fuel cell (HTFCs) the temperature value has a fundamental influence on the behaviour and on the design of the system. Talking about fuel cell, since energy is always produced the reaction are spontaneous ( $\Delta g_{react} < 0$ ) but if high temperatures can constitute an help for transport phenomena inside the cell, on the other hand it can constitute a relevant cost. In general, we can analyze the positive and negative effects of high operating temperatures as shown in the following list:

- ✓ Transport phenomena improvement – Charge transfer, ion conduction, mass transfer;

- ✓ No need of precious catalyst – Transport phenomena improvement make useless the need of catalyst as in PEMFC since the low operational temperature;
- ✓ Fuel flexibility – Since there is no precious catalyst sensible to carbon-based molecules a wide range of fuels can be used:
  - Hydrogen
  - Hydrocarbons ( $C_nH_m$ )
  - Alcohols
  - Ethers
  - Biogas
  - Syngas
- ✓ High temperature heat as by-product – Waste gases can find many different uses in industry;
- X No dynamicity – To reach operational temperature a certain time is requested and transients are not so fast as PEMFC. Mainly for this reason this kind of technology are not suitable for automotive applications and useful for power production to cover base loads avoiding thermal cycle;
- X Auxiliary materials – Low quality materials can be damaged by thermal stress so it turns in higher costs for auxiliary equipment.

While in PEMFC the electrolyte was a proton conductor material, in SOFC the ion conducted is the one generated by the reduction of the oxidant which is oxygen, so  $O^{2-}$ . As from the name of the involved technologies, the electrolyte is made of solid oxides which can be one or a mixture of them. The most used is the so called Yttria Stabilized Zirconia YSZ. It is composed of Zirconia Oxide ( $ZrO_2$ ) and Yttria Oxide ( $Y_2O_3$ ). It shows good quality in terms of ionic conductivity due to the doping of  $Y^{4+}$  with  $Zr^{3+}$  that cause  $O^{2-}$  vacancies in the lattice and thus free position to take by the migrating  $O^{2-}$  ions. Yttria stabilized zirconia does not result so expensive for SOFC and this is mainly due to the relevant presence in nature of Zirconia, while Yttria is not a so common material, but it is used just as dopant. The drawback of YSZ is the thermal behaviour of the ionic conductivity and ohmic resistance which show enhanced values only at high temperatures. In figure 2.4 the trend of the latter is shown. The anode is the phase where the oxidation of the fuel takes place to deliver electrons useful for the power generation.



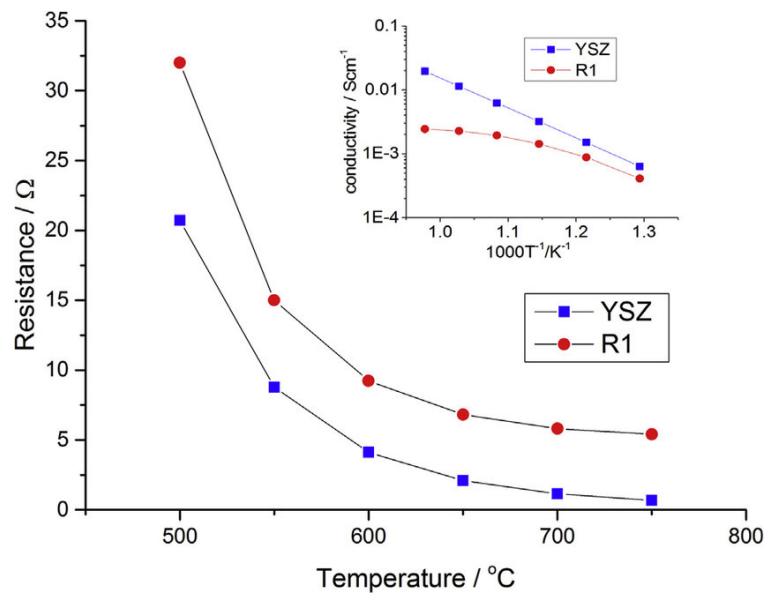


Figure 2.4 - Ohmic resistance for R1 and YSZ as a function of temperature [6]

SOFCS usually are anode-supported cells (ASC) therefore it has the biggest thickness (in the range  $250\div 500 \mu\text{m}$ ) and the best mechanical stability. Furthermore, anode must be a porous material allowing the diffusion of the fuel so it must have an electronic conducting phase and a ions one. The points where these two phases meet, which constitute the third phase, are the points where the anode semi-reaction occurs, called Three Phase Boundary (TPB). Ionic phase is made of the same material of the electrolyte, YSZ, since it must carry the  $\text{O}^{2-}$  ions to the TPB. Electronic conducting phase is made of Nichel, which gives to the anode also a metallic component. For this reason anode is also known as CERMET material, CERamic and METal. Nichel is inserted into anode by percolation so it can constitute a way for electrons to reach the interconnector. The cathode is made again in ceramic material, in particular is used a mix of different ceramic materials. This family is called MIEC that stands for Mixed Ionic Electronic Conductors since the aim of such conductors is to conduct  $\text{O}^{2-}$  ions to the electrolyte and electrons to the oxygen molecules. The most used is Lanthanium-Strontium-Manganite oxide, LSM, since it has the closest volumetric coefficient variation with the temperature with respect to YSZ. The LSM works well as a cathode at very high temperatures and very poorly at operating temperatures below  $800 \text{ }^\circ\text{C}$ . Molecular lattice of this material is called Perovskite which structural formula is  $\text{ABO}_3$  (Figure 2.5) and it is particularly famous in the field of material structure.

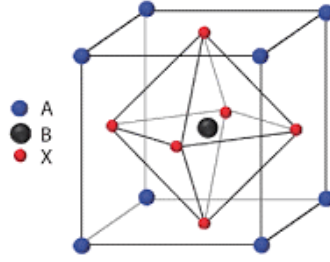


Figure 2.5 - Perovskite structure

Volumetric coefficient of the interconnector of the fuel cell has to be as similar as possible to that of YSZ in order to avoid mechanical stress and so possible cell breaking because of different structural behavior at high temperatures. Furthermore, interconnectors have to be tight to the molecules of the electrodes and good electronic conductor. The material which better satisfy these requests and mostly used for interconnectors is CROFER22APV. It is a metallic material composed by iron and 22% of chromium, which is a particular kind of stainless steel. The general formulation of the polarization curve of a fuel cell can be expressed as:

$$\begin{aligned}
 Vc(i) &= E - \eta_{ACT_{an}}(i) - \eta_{ACT_{cat}}(i) - \eta_{OHM}(i) - \eta_{DIFF_{cat}}(i) - \eta_{DIFF_{an}}(i) = \\
 &= \frac{RT}{z_F F} \ln \left[ \frac{\prod_R \left( \frac{p_i}{p_o} \right)^{v_R}}{\prod_P \left( \frac{p_i}{p_o} \right)^{v_P}} \right] - \frac{\Delta \bar{g}_{react}(T, p_0)}{z_F F} - \frac{RT}{n_{RDS} F \beta} \sin^{-1} \left( \frac{i}{2i_{0_{an}}} \right) - \frac{RT}{n_{RDS} F \beta} \sin^{-1} \left( \frac{i}{2i_{0_{cat}}} \right) \\
 &\quad - ASR i - \left[ -\frac{RT}{z_{an} F} \ln \left( 1 - \frac{i}{i_{e_{an}}} \right) \right] - \left[ -\frac{RT}{z_{an} F} \ln \left( 1 - \frac{i}{i_{e_{cat}}} \right) \right]
 \end{aligned}$$

Since the high temperature helps transport phenomena, the relative voltage drops depending directly on the materials used for electrodes and electrolyte are very low and so negligible. Therefore, the formulation of the fuel cell polarization curve can be simplified in:

$$Vc(i) = E - \eta_{OHM}(i) = E - ASR i = \frac{RT}{z_F F} \ln \left[ \frac{\prod_R \left( \frac{p_i}{p_o} \right)^{v_R}}{\prod_P \left( \frac{p_i}{p_o} \right)^{v_P}} \right] - \frac{\Delta \bar{g}_{react}(T, p_0)}{z_F F} - ASR i$$

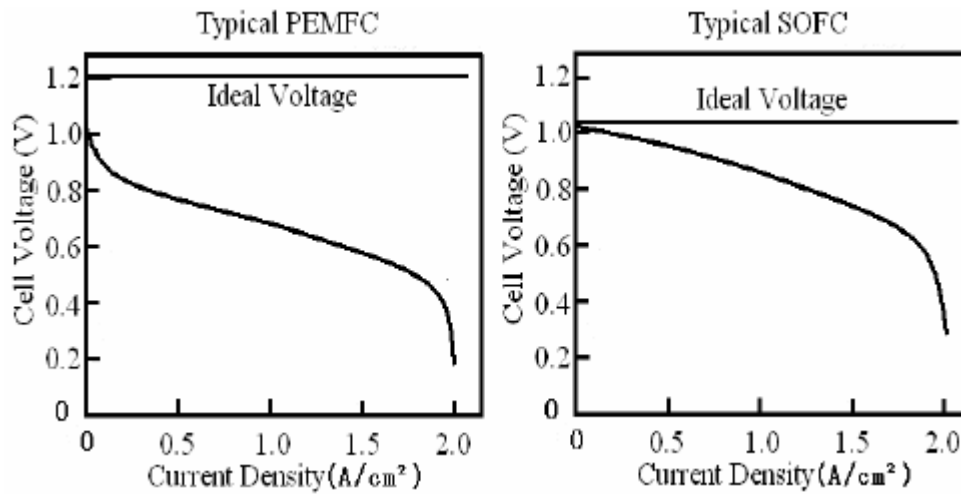


Figure 2.6 - PEMFC and SOFC performance comparison [7]

In Figure 2.6 characteristic operating curves of PEMFCs and that of SOFCs are compared, and it can be seen that:

- The open circuit voltage OCV of PEMFCs is higher than SOFCs one;
- Slope of PEMFC is higher than SOFCs one which means that a higher value of ohmic losses in the former;
- Activation and diffusion over-voltage in PEMFCs are not negligible while they are in SOFCs;
- PEMFC curve is almost always under the SOFC one.

As is the case of PEMFC, it can also happen in SOFC that particular operating conditions can lead to the deposition of carbon atoms on the electrode lattice generating problems for cell operation.

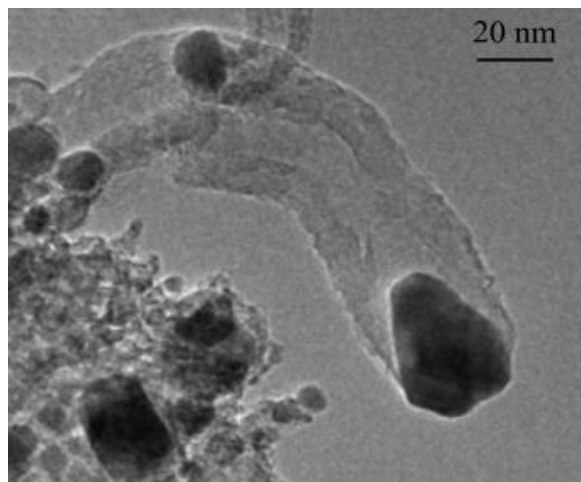


Figure 2.7 - Carbon whisker [8]

Carbon atoms produced by the degradation of fuels like methane ( $\text{CH}_4$ ) and carbon monoxide ( $\text{CO}$ ), deposits in solid state on the walls of the pores of the anode organizing in a series of whiskers (Figure 2.7), micro-strands of carbon without defects. Whiskers mass growing generates a thick skein which acts as stopper causing pores closing. Since the fuel cannot pass through the pores, it cannot reach the grains of the catalyst. This mechanism is called Whisker mechanism and explains the increasing of impedance at high frequency value over time. Since the pores are closed by carbon skein and no fuel can reach the catalyst to be reduced by the oxygen ions that continues to arrive from the electrolyte, the ions oxidise the catalyst producing Nickel oxide ( $\text{NiO}$ ). The latter has a higher volume than the metallic Nickel, which means a pressure generated on the surrounding molecules. Pressure generates high static force and tension inside the structure of the anode and of the electrolyte which are made of ceramic material (YSZ). Therefore, the carbon deposition inside the anode leads to the cell breaking. Moreover, all this sequence of events happens at very high temperature and a sudden contact between fuel and oxidant can causes fire or cell melting. To avoid Whisker's phenomenon a stable mixture of fuel has to be generated, an adequate mix of hydrogen, carbon and oxygen mole fraction permits to avoid the degradation reaction of C-fuel molecules. The Equilibrium C-O-H triangle (Figure 2.8) is a diagram that reports on its axis the mole fraction of C, H and O and a line sign the area in which the related composition of the mixture leads or not to the carbon deposition. It is based and built on thermodynamic considerations so the limit composition line change on the base of temperature and pressure conditions.

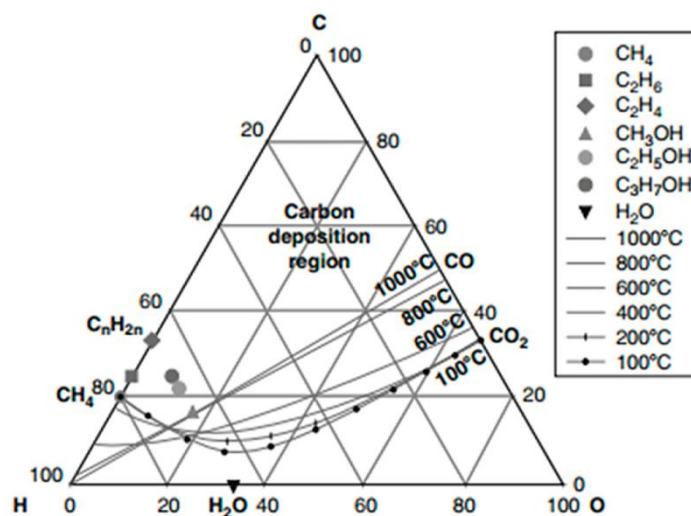
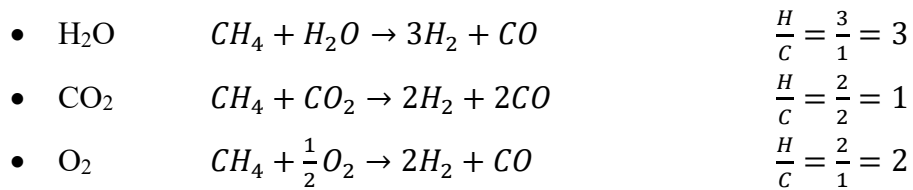
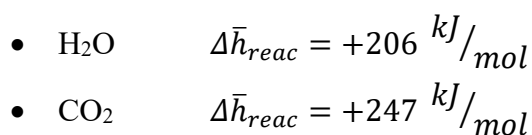


Figure 2.8 - Carbon deposition limit boundaries for a C-H-O composition for various types of hydrocarbons [9]

It is possible to avoid carbon deposition generating a stable mixture of fuel by the addition to it of an oxygen carrier. Indeed, the oxygen is necessary to bond carbon that otherwise will remain an isolated product of the reaction. Many molecules can act as oxygen carriers but the most used because of their simplicity, availability and affordability are water, carbon dioxide and oxygen. The choice must be done considering both the ratio H/C and the thermal management considerations. One parameter to choose the best oxygen carrier is the amount of hydrogen produced as real fuel starting from the filler one. Richness in hydrogen can be determined directly by the stoichiometric reactions involving the carriers and the starting fuel by evaluating the ratio H/C. The higher is the ratio the higher will be the quality of the secondary fuel and so of the carrier. Considering methane as filler fuel:



The best carrier in terms of quality of the fuel is water followed by oxygen, while the worst is the carbon dioxide since it carries also carbon. Thermal management of SOFCs stack is provided by a huge air amount. Since the combustion of carbon-based molecules directly with oxygen is an exothermic reaction, consider oxygen as a carrier leads to the necessity of further amount of air to cool the machine and an increase of auxiliary losses and so a decrease of global efficiency.



Both the carriers are involved in endothermic reactions, means that the stack would be provided of a sink of heat, decreasing the amount of air required to cool down the stack. Furthermore, a comparison between the use of methane with respect to hydrogen as fuel highlights that even if the cell fuelled with hydrogen is electrochemically more efficient, the one fed by methane is more efficient because of the heat sink in the anode which decreases auxiliary losses increasing global efficiency. Considering both the observation on the hydrogen to carbon ratio and on the thermal management, the best carrier to provide oxygen availability is H<sub>2</sub>O which allows the production of a very high quality secondary fuel and provide a sink for the heat management of the stack.

## 2.2 Organic fraction of municipal solid waste treatment and recovery plant

The spread of separate waste collection has facilitated the net reduction of gases produced by landfilling of waste. Last years a decline in the amount of waste sent to landfills was observed, in favour of the recovery of materials and energy from them so in line with the circular economy concept. The latter has changed waste management, stimulating the growth of new technologies and markets. Organic fraction of municipal solid waste (OFMSW) treatment plant produces biogas and high-quality compost through an anaerobic digestion process. After an upgrading process a mixture of methane (50-75%), carbon dioxide (25-45%), hydrogen and other compounds can be obtained. Biomethane is a renewable gas with the same characteristics of natural gas, so it can be injected to the national gas distribution grid without the necessity of relevant investment costs.

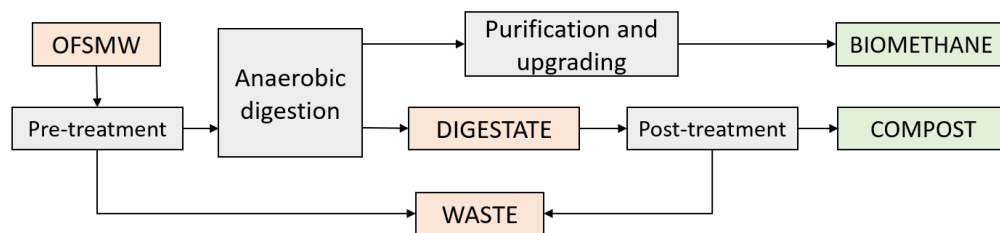


Figure 2.9 - OFMSW treatment process scheme

Biomethane and production process can be summarised in the following steps:

- Pre-treatment – Initial phase where the waste undergoes operations to remove unwanted contaminants such as plastics, metals, and other non-biodegradable materials;
- Anaerobic digestion – The treated organic fraction is sent to an anaerobic digestion reactor. In this oxygen-free environment, microorganisms degrade the organic matter, producing biogas, composed mainly of methane (CH<sub>4</sub>) and carbon dioxide (CO<sub>2</sub>);
- Upgrading – Biogas must be purified by carbon dioxide and other compound trace (NH<sub>3</sub> and H<sub>2</sub>S) before being compressed and injected to the grid;
- Digestate post-treatment – The water content in digestate must be reduced by mixing with dry structurant (wood) and then it can be submitted to the aerobic treatment to become compost.

The most common types of OFMSW anaerobic digestion of organic matrices are WET and DRY:

- WET – The matrix to be fed is finely crushed and added to water in order to produce a puree;
- DRY – The matrix to be fed is only separated from the inorganic fractions (plastics, metals, and aggregates) without addition of water

Main advantages and disadvantages of the above-mentioned technologies are shown in table 2.2.

*Table 2.2 - Advantages/Disadvantages anaerobic technologies DRY and WET*

| <b>TECHNOLOGY</b> | <b>PROs</b>  | <b>CONs</b>   |
|-------------------|--|---|
| DRY               | <ul style="list-style-type: none"> <li>• Simplified pretreatment</li> <li>• Smaller digester volumes</li> <li>• Lower volumes of leachate to be treated</li> </ul> | Expensive process   |
| WET               | Most popular technology  | <ul style="list-style-type: none"> <li>• Complex pretreatment</li> <li>• Larger digester volumes</li> <li>• Smaller digester volumes</li> </ul> |

Because of the lower energy costs, easier and lower wastewater management, less space occupied by digesters so lower visual impact, the decision was made to adopt DRY technology. Two types can then be identified among DRY technologies, batch systems, where digesters process waste in batches and are alternately filled and then completely emptied using operating means such as wheel loaders, and plug-flow systems, which instead are loaded and unloaded continuously using automated systems. The first are cheaper but manage to achieve lower performance in terms of organic matter to biogas conversion efficiency and require constant intervention by operating personnel inside the digesters, with potential health and safety issues, so plug-flow technology was chosen.

The choice of biogas upgrading technology was made after evaluating the environmental, technological and economic impacts related to the main established technological alternatives in Italy and Europe, which can be grouped into the following technological strands:

- Amine scrubber;
- Membranes;
- Pressure Water Scrubbing (PWS);
- Pressure Swing Adsorption (PSA).

Table 2.3 summarizes the pros and cons of each solution.

*Table 2.3* - Upgrading technologies Advantages/Disadvantages

| <b>SOLUTION</b> | <b>PROs</b>  | <b>CONs</b>   |
|-----------------|--|---|
| Amine scrubber  | <ul style="list-style-type: none"> <li>• Maximum CH<sub>4</sub> recovery efficiency</li> <li>• Low electrical consumption</li> </ul> | <ul style="list-style-type: none"> <li>• High thermal consumption</li> <li>• Use of compounds (amines) that are potentially hazardous to health</li> <li>• High sensitivity to H<sub>2</sub>S and other compounds presence</li> </ul> |
| Membranes       | <ul style="list-style-type: none"> <li>• Simple design</li> <li>• Modularity</li> </ul>  | <ul style="list-style-type: none"> <li>• High electrical consumption</li> <li>• CH<sub>4</sub> recovery efficiency lower than competitors</li> <li>• High sensitivity to H<sub>2</sub>S and other compounds presence</li> </ul>       |



|     |   |   |
|-----|---|---|
| PWS | <ul style="list-style-type: none"> <li>• Good CH<sub>4</sub> recovery efficiency</li> <li>• Low sensitivity to H<sub>2</sub>S and other compounds presence</li> <li>• No hazardous additives use</li> </ul> | <ul style="list-style-type: none"> <li>• Mid-high electrical consumption</li> <li>• Production of liquid effluent to be disposed</li> </ul>                               |
| PSA | <ul style="list-style-type: none"> <li>• Low electrical consumption</li> </ul>  | <ul style="list-style-type: none"> <li>• Mid-low CH<sub>4</sub> recovery efficiency</li> <li>• High sensitivity to H<sub>2</sub>S and other compounds presence</li> </ul> |

Due to the robustness, high number of references, high CH<sub>4</sub> recovery efficiency, low environmental impact, considering that no environmentally and health hazardous chemical additives are used, pressurized water scrubber (PWS) technology was chosen.

### 2.2.1 Anaerobic digestion process

Anaerobic Digestion is a special treatment process in which, in sealed tanks, anaerobic microbial strains are selected (by inoculation and subsequent maintenance), which provide for the transformation of organic matter into biogas. Biogas is a gaseous mixture consisting mainly of methane (55-65% by volume) and carbon dioxide. The process operates on all organic substrates such as agro-food waste, biomass from agricultural sources, industrial organic residues and the organic fraction from separate collection of municipal solid waste (OFSMW). Biogas production yield is expressed as the amount of biogas produced per unit of organic material fed and, for the above organic matrices, is generally between 90 and 200 Nm<sup>3</sup>/t. The anaerobic digestion process is active within a wide temperature range of -5 to 70 °C. Based on temperature, the process is called:

- Psychrophilic if it occurs at temperatures below 20 °C;
- Mesophilic if it occurs at temperatures between 20 and 40 °C;
- Thermophilic if it occurs at temperatures above 40 °C.

Generally, the anaerobic process is divided into 3 stages: hydrolysis and acidification, acetogenesis and methanogenesis.

### *Hydrolysis and acidification*

In this first stage specific anaerobic bacterial strains degrade complex carbohydrates into carbohydrates simple, proteins to peptides and amino acids, and fats to glycerol and fatty acids. Finally, they degrade the newly formed monomers by producing volatile fatty acids.

### *Acetogenesis*

In the second stage, the hydrolysis and acidification products are metabolized by other bacterial strains specific which transform them into acetic acid, formic acid, carbon dioxide and hydrogen.

### *Methanogenesis*

The third and final stage of the anaerobic process is methane production. Methane production occurs through two different types of reactions: methanogenesis by hydrogenotrophic bacteria, which anaerobically oxidize hydrogen and carbon dioxide, and production acetoclastic with formation of methane and carbon dioxide. Most methane production occurs through the second mechanism.

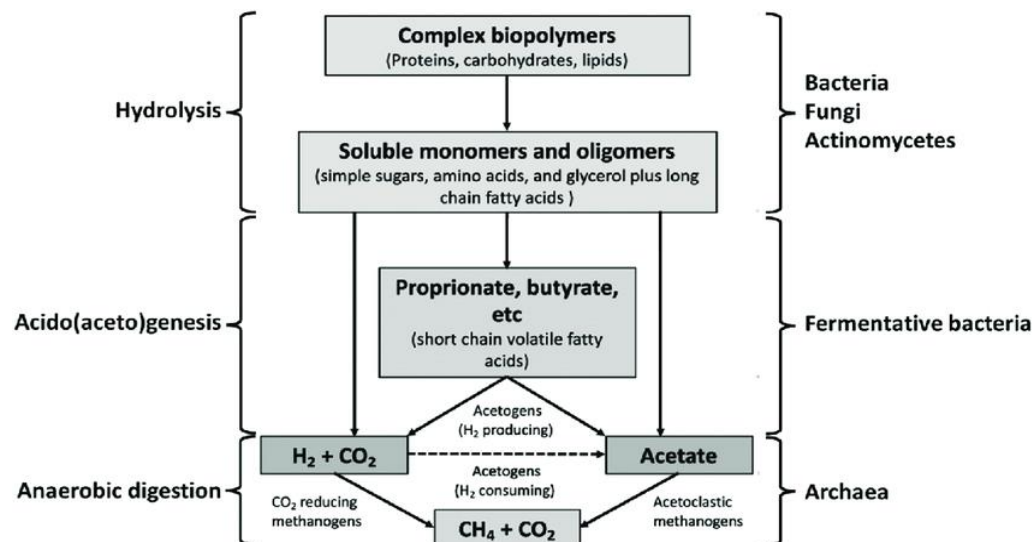


Figure 2.10 - Steps of the methanogenesis process [10]

For the good management of the reaction:

- The matrix to be degraded anaerobically (ingestate) should usually be characterized in terms of total solids (TS), volatile solids (TVS), chemical oxygen demand (COD) and biological oxygen demand (BOD);

- The output material from digestion (digestate) should usually be characterized in terms of COD and BOD.

### 2.2.2 Composting process

The composting process is well known in the literature and widespread in Italy and Europe. This consists of an aerobic process of biological decomposition of organic matter that takes place under controlled conditions, which makes it possible to accelerate and improve the natural process to which any organic substance undergoes because of the microbial flora naturally present in the environment. The product of this process (compost) is particularly rich in humus, in active microbial flora and in microelements.

The composting process essentially consists of two stages:

- accelerated bio-oxidation (or ACT phase, active composting time), in which there is sanitization of the mass: this is an active phase characterized by intense processes of degradation of the most easily degradable organic components.
- maturation during which the product is stabilized by enriching itself with humic molecules.

In the specific case of the proposed plant, the aerobic treatment phase is preceded by an anaerobic phase, which degrades much of the putrescible organic components, which means that the former must operate on a material that has already been pretreated, which therefore requires a lower residence time than those provided by conventional composting plants.

### 2.3 SOFC & OFMSW

Biogas is one of the most popular renewable fuels. It is currently used for power and heat generation with conventional systems, but an alternative and more sustainable use is possible with solid oxide fuel cells (SOFCs). The composition of biogas depends on the source substrate but basically consists of 50-75% (CH<sub>4</sub>), 25-45% (CO<sub>2</sub>), 2-7% (H<sub>2</sub>O) at 20-40 °C, about 2% (N<sub>2</sub>), less than 1% (H<sub>2</sub> and H<sub>2</sub>S) and traces of O<sub>2</sub>, NH<sub>3</sub>, halides and siloxanes [11]. The trace compounds existing in biogas can present a significant challenge to its energetic use. Sulphur compounds in concentrations of few ppm<sub>v</sub> (or even ppb<sub>v</sub>) can significantly degrade any catalytic process which use biogas. In recent years there has been a

focus on the use of biomass-derived fuels in fuel cells in combination with pre-reforming processes. The use of fuel cells in this area for stationary applications appears to be promising because of their high efficiency, drastic reduction in pollutant emissions, absence of moving parts and thus low noise level, and modularity that allows different power sizes to be installed without significant variations in efficiency. Solid oxide fuel cells (SOFCs) are more advantageous because the high operating temperatures allow thermal integration of the stack with all the conversion (reforming) and biogas purification steps necessary to increase system efficiency and lifetime. In addition, the high-temperature heat as a by-product can be used to meet the thermal needs of the digester, ensuring that efficiencies of 80 to 90 percent are achieved.

On other hand, SOFCs are indeed more sensitive to various types of impurities typically founded in biogases, including sulphur, silicon and chlorine compounds. For this reason, impurities should be removed at very low levels (typically <1ppm) to ensure a safe environment as the fuel cell anode [12]. Even though the purification unit is recognized in many literatures works as a critical aspect in biogas SOFC plants, there are few analyses that specifically address the deep purification of biogas for use in fuel cell. Raw biogas often contains significant amount of undesirable trace compounds such as hydrogen sulphide and siloxanes [13], molecules which can lead to SOFC degradation even at low concentrations. Various biogas purification systems for conventional CHP plants are available on the market, for upgrading biogas in biomethane or for contaminants removal. Biogas upgrading by means of pressure swing adsorption, water/chemical scrubbing and membranes, completely removes the impurities to meet the requirements of the natural gas grid.

### 3. ASPEN Model

#### 3.1 SOFC layout

Aspen Plus V10 was used to simulate the process, fragmenting the fuel cell stack as a function of the physical and chemical transformations that take place within it. The main objective is to identify the characteristic parameters of the system to evaluate the electrical and thermal production of the fuel cell and identify the size according to the existing models on the market.

In a general diagram shown in Figure 3.1 it is possible to identify three main flows:

- Natural gas – anode side – Fuel of the stack, after an initial compression and heating phase, passes through reformer and anode at the exit of which a part is recirculated while the rest reaches the afterburner;
- Air – cathode side – Oxidizer of the reaction, it is compressed and heated before reaching the cathode and afterburner;
- Exhaust gases – Outlet stream – A mixture of gases, composed of  $\text{CO}_2$ ,  $\text{H}_2\text{O}$ ,  $\text{N}_2$  and  $\text{O}_2$ , which can provide the heat useful for the thermal needs of the stack but also for heat recovery outside the module.

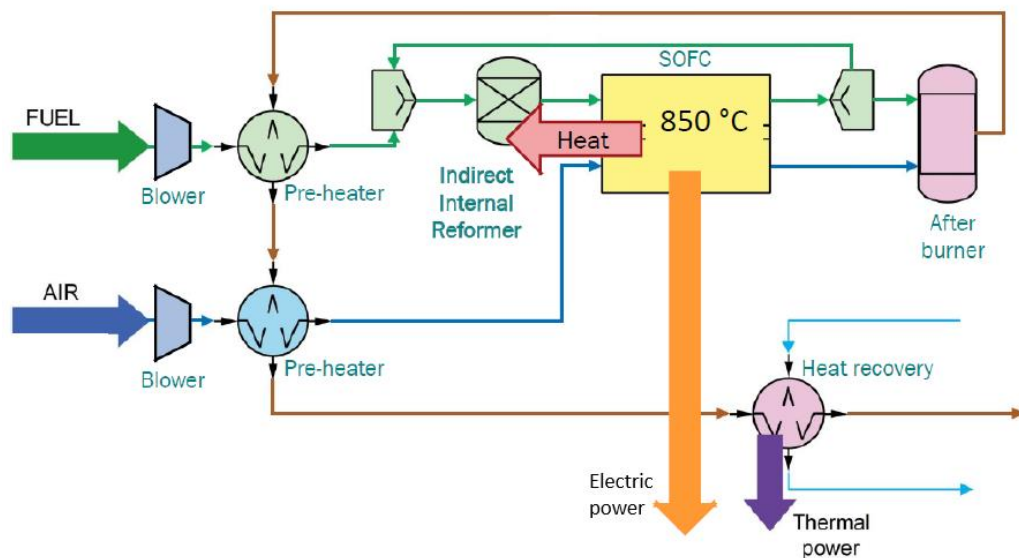
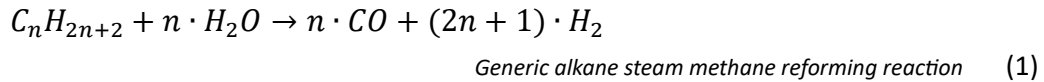


Figure 3.1 - SOFC ASPEN layout

A methane reformer is a device based on steam reforming, autothermal reforming or partial oxidation and it is a type of chemical synthesis which can produce pure hydrogen gas from methane using a catalyst, according to the type of oxidant used. There are several types of reformers nowadays in development but the most common in industry is Steam methane reforming (SMR).



The CO produced can react further producing H<sub>2</sub> by the water-gas shift reaction (WGS).



The steam reforming reaction is highly endothermic (e.g. for CH<sub>4</sub> Δ<sub>h<sub>r</sub></sub> = 205.84 kJ/mol), while the water-gas shift is moderately exothermic (Δ<sub>h<sub>r</sub></sub> = -41.17 kJ/mol). Both require a catalyst. On Ni/YSZ anode, the coupling of the fast endothermic reforming reaction with the sluggish exothermic electrochemical oxidation can generate severe instabilities. An excess of steam is typically required to prevent carbon deposition by promoting the water-gas shift reaction and reduce the partial pressure of CO. In typical SOFC, the reforming step is done after the desulphurization using an external unit. This type of design is suitable for large-scale system with combined heat and power generation and is known as external reforming SOFC. For small-scale application the complexity and size of the overall system can be reduced by eliminating the external reformer and annex unit and reforming the fuel inside the stack. The latter design is known as internal reforming and uses the waste heat generated by the electrochemical oxidation and other non-reversible process to offset the heat requirements of the reforming reactions [14]. Internal reforming can be achieved either indirectly, using a dedicated reforming catalyst inside the SOFC stack, or directly on the Ni/YSZ anode. Indirect internal reforming is simpler and cheaper than external reforming, but it can be difficult to adjust the reforming reaction to the electrochemical oxidation so that most of the fuel is converted into synthesis gas without residual fuel reaching the anode.

### 3.2 SOFC Anode

Anode is fed by fuel, in this study biogas exiting the cleaning system with a theoretical chemical composition of 60% of CH<sub>4</sub> and 40% of CO<sub>2</sub>. Aspen model of the anode side consider a series of few devices which simulate the functioning of that part of the stack. First, a fuel blower is necessary to compress the biogas flow increasing the pressure of 200 mbar. Compression is needed to compensate pressure losses due to the whole system. However, the fuel flow needs to be pre-heated before entering the reformer, which works at a temperature of about 800

°C, and this is done by means of a heat exchanger which transfer part of the thermal power inside the outlet stream to the biogas, increasing its temperature. This process is used to produce pure hydrogen from methane through to the steam methane reforming reaction. The steam for the reforming process will be provided through the partial anode recirculation which recirculate part of the anode exhausted gases into reformer. The recirculation must be done only with the strictly necessary amount of exhaust because of the unreacted CO, that increase the carbon amount at the anode, and the decreasing of the partial pressure of the fuel which decreases the  $\Delta V$  of the cell according to the Nernst equation. Recirculation mode is a very important question for the efficiency point of view since an active recirculator means an increasing auxiliary loss so a decrease of the global efficiency. Moreover, the installed blower should work in dangerous conditions due to the high temperature and the presence of residual H<sub>2</sub> and CO. The best solution found is the use of an ejector which is cheap and not electrically driven. It is a convergent-divergent nozzle installed in the conduct of the inlet mixture at the stack anode which generates an increase of the stream velocity and so a little depression which aspirates recirculating gas in the main pipe. The simulation of the anode recirculation on Aspen has been modelled by means of a splitter, after the SOFC anode which separates the exhausted gas, and a mixer placed before the reformer, to dilute the fresh biogas flow (Figure 3.2).

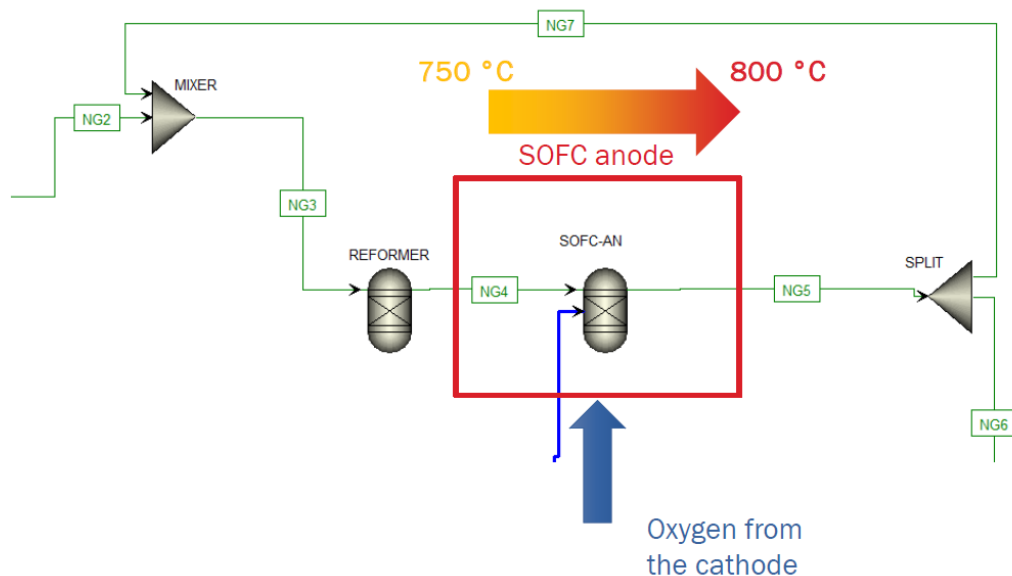
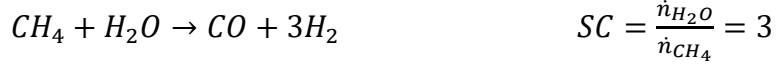


Figure 3.2 - Anode recirculation loop

The split ratio to set on Aspen is linked with the steam to carbon ratio (S/C). It is the ratio of moles of steam to moles of carbon in the reformer feed. It is obtained by dividing the molar flow rates of steam and feed. The reformer feed must contain sufficient steam to avoid cracking of the hydrocarbons and coke

formation. An excess of steam (over stoichiometric ratio) is usually used. The higher the steam to carbon ratio, the lower the residual methane will be for a given reformer outlet temperature. Hence, less energy is required in the furnace. The design steam to carbon is typically 3.0 with a range between 2.5 and 5.0 [15].



The reformer and the SOFC have been modeled as a Gibbs equilibrium reactor working respectively at 800 °C and 850 °C. Calculator input block (C-INPUT) on Aspen performs calculations with variables imported from the flowsheet or generated within the block. Some of that can be exported to the flowsheet, they can be used by other blocks. C-INPUT variables are Biogas flow rate (NFUEL), SOFC current in nominal condition (CTOT) and stoichiometric oxygen (NOXY).

- $\dot{M}_{fuel} [kg/h] = \dot{V}_{fuel} [m^3/h] \cdot \rho [kg/m^3]$
- $\bar{n}_{fuel} [mol/s] = \dot{M}_{fuel} [kg/h] \cdot 1000 [g/kg] \cdot \frac{1}{3600 [s/h]} \cdot \frac{1}{Molar\ weight [g/mol]}$
- $I_{tot} [A] = \bar{n}_{fuel} [mol/s] \cdot 8 \cdot F \cdot FU \cdot \%CH_4$
- $\bar{n}_{O_{2stoich}} [mol/s] = \frac{I_{tot}}{4 \cdot F}$

Table 3.1 - Biomethane parameters

|                          |      |                           |
|--------------------------|------|---------------------------|
| $\dot{V}_{fuel} [m^3/h]$ | 270  | Biomethane flow rate      |
| $\rho [kg/m^3]$          | 1.2  | $CH_4-CO_2$ 60% – 40%     |
| $Molar\ weight [g/mol]$  | 27.2 | $CH_4-CO_2$ 60% – 40%     |
| FU [%]                   | 70   | Fuel utilization          |
| $CH_4\%$                 | 60   | Methane content in biogas |

A design specification (DS) is a tool of Aspen which allows to define a setpoint and define a second variable which will be changed by the DS tool, in a range defined by the user to meet the desired set point on the first variable. In the SOFC model a define specification is used to define the steam to carbon ratio.



A target ratio is fixed (SC=3) to guarantee enough water and avoid carbon deposition problems. The variable to be changed will be the split fraction of the splitter, adjusting the water to recirculate back to the reformer.

### 3.3 SOFC Cathode

At the beginning air flow is compressed and then pre-heated. Through heat exchangers the thermal power produced by the stack is removed to keep the Gibbs equilibrium reactor (SOFC system) temperature constant.

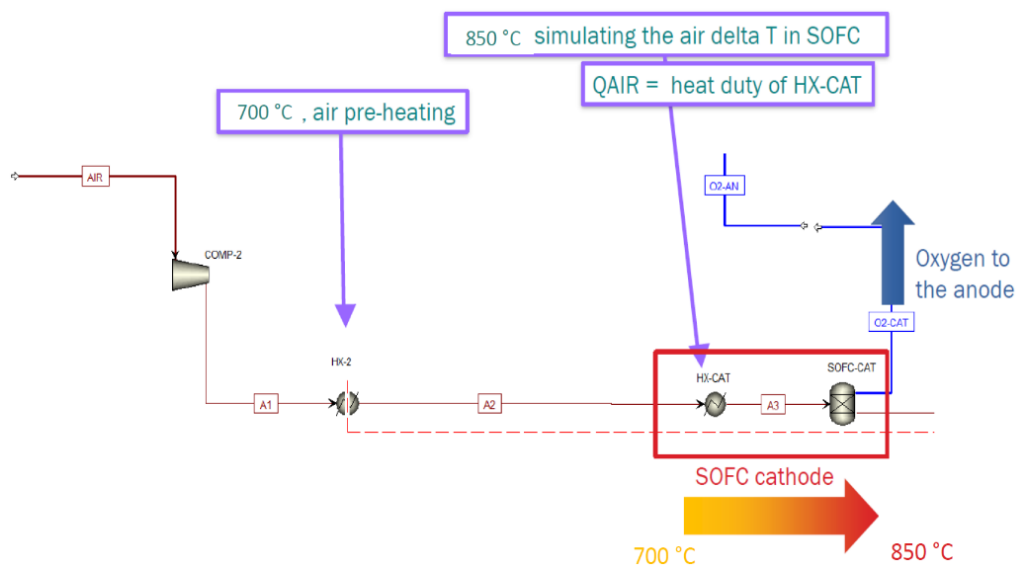


Figure 3.3 - Cathode air heat exchange

The cathode side air flow provides the amount of oxygen required to convert all the input fuel flow. On Aspen this value is determined inside C-INPUT calculator block. The same amount should be extracted by the air, so it is exported by means of a Separator block. Another calculator block (C-OXY) is needed to overwrite the oxygen required from the cathode.

$$\bar{n}_{O_{2AN}} = \bar{n}_{O_{2CAT}}$$

### 3.4 SOFC heat recovery and pre-heating system

The high operating temperatures of the SOFC stack along with the production of thermal power by the stack itself highlights the importance of thermal management of the system. The way to maintain temperature and remove excess heat produced is to blow a large excess of air to the anode. The amount of air required by the reaction is the stoichiometric one.

Air Utilization (AU) express the ratio between the stoichiometric air and the total one. Air excess  $\lambda$  is the reciprocal of AU. Value of AU related to SOFC stack system working with methane as fuel is usually the 20%, that means a value of  $\lambda$  of about 5. Huge flow of air requires powerful blowers to be provided which consumes big amounts of electrical energy consumed by auxiliaries, strictly related with a decrease in global efficiency. Air excess ratio is determined from the thermal balance of the SOFC system. The objective is to remove the heat produced by the SOFC exothermic reaction, dissipating some of it to supply endothermic reforming reactions, and the other fraction is removed from the air. Calculator block C-AIR solves thermal balance and estimate the waste heat which should be exhausted from air flow. This parameter is exported as design specification DS-AIR.

- $\Phi_{react} = \Delta H_{react} - W_{el}$
- $W_{el} = V_C \cdot I_{TOT}$
- $\Phi_{AIR} = \Phi_{react} - \Phi_{REF}$
- $\Phi_{AIR} = \dot{m}_{AIR} \cdot c_{p,AIR} \cdot (T_{OUT,AIR} - T_{IN,AIR})$

Heat removed by the air flow is the thermal power exchanged in the cathode heat exchanger block (HX-CAT) on Aspen model layout (Figure 3.3).

- $\Phi_{waste} = \Phi_{air} = \Delta H_{react} - W_{el} - \Phi_{REF}$

Design specification overwrite air flow rate to set thermal power of HX-CAT equal to waste heat previously calculated. The recirculating flow of the exhausted from the anode is not the only thing that is done to save energy and reuse it within the system itself.

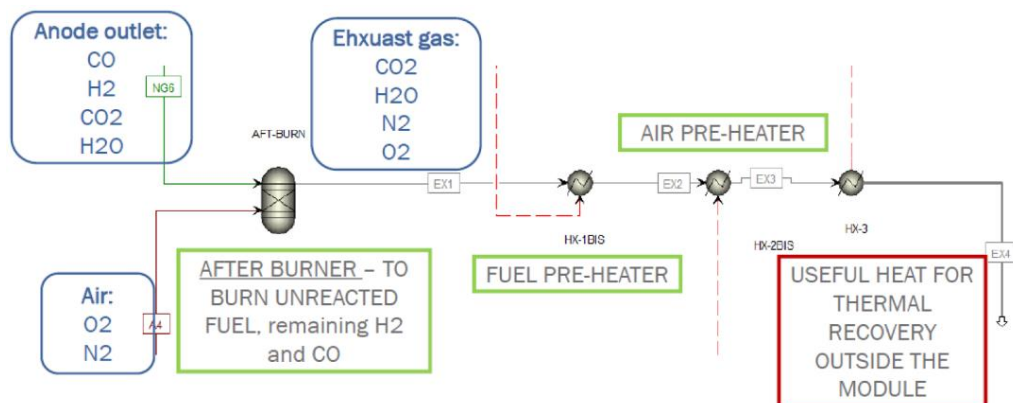


Figure 3.4 - Fuel cell thermal balance

Exhausted anode flow that is not recirculated in the anode inlet is still rich in hydrogen, carbon oxide and methane and can be burnt in an After-Burner with the exhaust flow from the cathode which is rich in oxygen. The heat generated slightly increases the temperature of the so formed final exhaust. The latter flow is used to preheat both the fuel, up to a temperature of about 800 °C, and cathode inlet air flux from 50 °C to about 600 °C because the air cannot be used on a cathode which is working at about 750 °C, volume variation due to temperature gradient could break the stack (Figure 3.4). Last heat exchanger (HX3) supplies the useful amount of thermal power which can be consumed outside the SOFC stack, to the end user within the plant. After setting all the blocks, inlet flow characteristics and some relations on Aspen, the simulation results, in terms of temperature, pressure and molar flow rate, are shown in Figure 3.5.

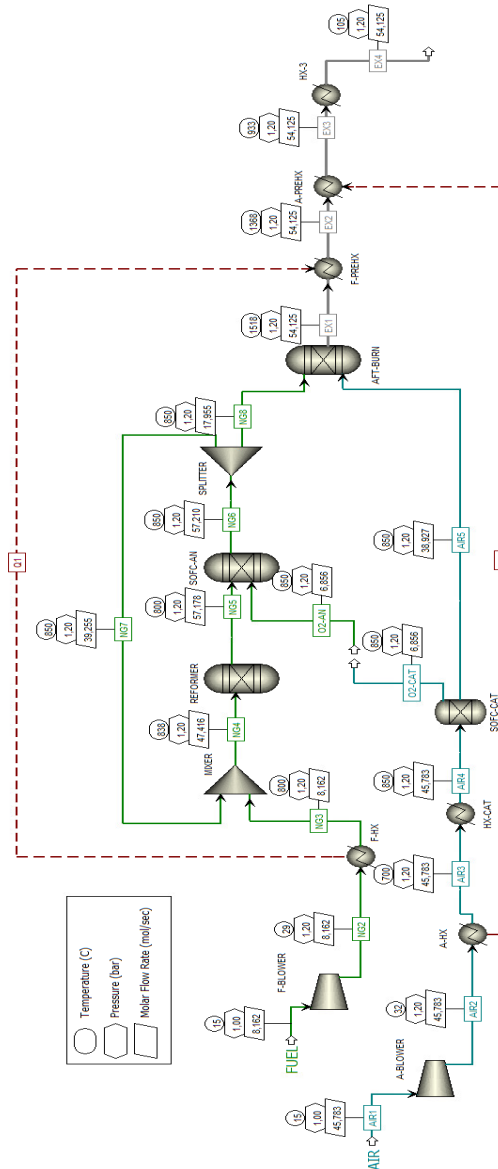


Figure 3.5 - Simulation results

## 4. Results

In order to carry out energy optimization of the municipal solid waste organic fraction treatment plant, it is necessary to identify the thermal and electrical demands required to operate the plant in the basic configuration. It is thus possible to carry out an initial economic analysis so as to identify the parameters that can be compared with the subsequent configurations analysed, that is, the one in which the boilers are replaced by a stack of fuel cells fired in the first case by natural gas taken from the grid and in the second and last case fired by a fraction of the biomethane produced by the biodigester.

### 4.1 Standard configuration

In the starting configuration, hereafter referred to as the "base case," two equal 780 kW boilers provide the total heat demand needed for the entire plant. The latter is transferred into two separate heat exchangers that feed the anaerobic biodigester and the biocells, respectively. The total thermal energy required by the plant annually, according to data from the technical report provided by A2A's engineering department [16], amounts to 5,5 GWh. The boilers are fed by natural gas withdrawn from the national distribution network. The annual consumption of natural gas withdrawn from the network, considering a maximum hourly flow rate of about 170 m<sup>3</sup>/h, amounts to 720,000 Nm<sup>3</sup> [16]. The unit gas price has been estimated by considering the average value of the GME day-ahead gas market for the period October 22/September 23 equal to 56,789 €/MWh. GME is the company responsible in Italy for organizing and managing the electricity, natural gas and environmental markets, as well as ensuring the economic management of adequate availability of energy reserves. A2A Ambiente department provided the unit cost for a 780 kW boiler equal to 75 k€, thus an amount equal to 150 k€ has to be considered since the power to be installed is equal to 1,56 MW. The annual consumption of electricity required to operate the anaerobic digestion plant, upgrading to biomethane and composting, will amount to approximately 8 GWh and will be roughly divided among the various plant sections as shown in the table below (Table 4.1) [16].

**Table 4.1** - Electrical consumption breakdown

|   | PLANT PROCESS STEP                           | Installed power [kW] | Consumption [kWh/year] |
|---|--|----------------------|------------------------|
| 1 | Receiving and pretreatment                   | 550                  | 750.000                |
| 2 | Anaerobic digestion                          | 300                  | 600.000                |
| 3 | Biomethane upgrading and grid injection      | 450                  | 2.250.000              |
| 4 | Aerobic treatment                            | 660                  | 1.650.000              |
| 5 | Digestate mixing and final refining compost  | 320                  | 350.000                |
| 6 | Capture, transport and exhausted air culling | 550                  | 2.400.000              |
|   | <b>TOTAL</b>                                 | <b>2.830</b>         | <b>8.000.000</b>       |

The unit electricity price has been estimated by the mean value of the GME day-ahead electricity market session of 04/01/2024 equal to 91,17 €/MWh. A plant preparation cost was assumed, which takes into account all the operations required for the equipment commission. For the boiler maintenance costs, a percentage of 2% of CAPEX was assumed. The reference tariff for incentives arising from the injection of biomethane into the natural gas distribution network was found from the Ministerial Decree Biomethane Production - DM 15/09/2022 and it is equal to 60,76 €/MWh. In this configuration, the entire amount of annual biomethane production ( $6 \times 10^6 \text{ Nm}^3$  [16]) is destined for injection into the natural gas grid. Table 4.2 summarizes all costs considered and assumed for the base case configuration.

**Table 4.2** - Base case configuration costs breakdown

| CAPEX             |                  | OPEX         |                    | INCOMES              |                    |
|-------------------|------------------|--------------|--------------------|----------------------|--------------------|
| Plant preparation | 200.000 €        | Natural gas  | 406.428 €          | Biomethane injection | 3.623.726 €        |
| Boilers           | 150.000 €        | Electricity  | 729.360 €          |                      |                    |
|                   |                  | Maintenance  | 7.000 €            |                      |                    |
| <b>TOTAL</b>      | <b>350.000 €</b> | <b>TOTAL</b> | <b>1.108.347 €</b> | <b>TOTAL</b>         | <b>3.623.726 €</b> |

Based on the costs listed above, an economic analysis was carried out to identify the net present value (NPV) at 15 years and the payback time (PBT). This time frame was selected because the incentive supply is guaranteed for 15 years, further evaluations will be done based on the political and energetical future scenario. The results are listed below:

- NPV<sub>5y</sub>                    4.762.086 €
- NPV<sub>10y</sub>                    11.275.520 €
- NPV<sub>15y</sub>                    16.356.640 €
- PBT                            2,99 years

The global efficiency can be calculated taking into account also the electrical demand and the operating hours of the system.

$$\eta_g = \frac{P_{boiler}}{\dot{V}_{fuel} \cdot PCI_{NG} + \frac{E_{el}}{h}} = 0.55$$

#### 4.2 Natural gas fed SOFC stack configuration

To replace gas boilers provided in the base configuration with a fuel cell stack, it is necessary to identify the correct size of the latter. Aspen Plus V10 provided results for each simulation in terms of all operating parameters and energy outputs ( $W_{el}$  and  $Q_{HR}$ ). The aim of the simulations was to gradually increase the hourly flow rate of natural gas taken from the grid until the thermal power output of the last heat exchanger, which is intended for external use with respect to the internal needs of the fuel cell, meet the thermal needs of the entire waste treatment plant. The flow rate required to meet the above requirements was approximately 380 cubic metres per hour, which equates to approximately 3,328,800 Nm<sup>3</sup> per year, assuming continuous operation. For natural gas withdrawn from the distribution network, the parameters in Table 4.3 were taken into account.

**Table 4.3** – Natural gas parameters

|                                    |                       |
|------------------------------------|-----------------------|
| %CH <sub>4</sub> -%CO <sub>2</sub> | 85-15                 |
| Fuel density                       | 0,9 kg/m <sup>3</sup> |
| Fuel molecular weight              | 20,2 g/mol            |

From the model built on Aspen, the electrical output of this fuel cell stack was calculated to be 1.4 MWe. Since both the natural gas compressor, which is needed to overcome the pressure drops generated within the fuel cell, and the cathode air fan are considered auxiliary utilities, their consumption must be deducted from the gross electrical power (Table 4.4). The net AC power of the fuel cell stack is therefore approximately 1.3 MWe.

**Table 4.4** – Natural gas fed SOFC configuration energy consumption and production

|                            |             |
|----------------------------|-------------|
| $W_{\text{fuel blower}}$   | 2.904 W     |
| $W_{\text{air blower}}$    | 39.513 W    |
| $Q_{\text{Heat Recovery}}$ | 632.315 W   |
| $W_{\text{net AC}}$        | 1.364.620 W |

Seven 200 kW modules were selected to accommodate commercially available electrical sizes. However, in the economic analysis, an additional 200 kW module was added (8x200 kW total) to cover periods of maintenance, either ordinary (stack replacement) or extraordinary, to still provide the power required to operate the municipal waste treatment plant, as it is a continuous operation. Because no well-defined value can be identified with certainty for the unit cost of fuel cells, a sensitivity analysis was performed in a price range from 2 to 10 k€/kW. To clearly show the breakdown of costs, the values below refer to the unit cost of 3 k€/kW. For the general maintenance costs, a percentage of 2% of CAPEX was assumed. Stack replacement is one of the most important OPEX. It should be carried out every 5 years and has a cost of about 30% of the initial cost of the SOFC. The heat provided by the fuel cell flue gas is exchanged through an appropriate heat recovery system. In order to identify a reference price, a scaling factor was used starting from a known price for a given power output.

$$C_{HR} = C_0 \cdot \left(\frac{S_1}{S_0}\right)^n$$

- $C_{HR}$  Thermal recovery system cost
- $C_0 = 50.000 \text{ €}$  Heat recovery system investment cost for  $S_0$  size
- $S_1 = 632,315 \text{ kWt}$  SOFC thermal power
- $S_0 = 90 \text{ kWt}$  Reference size
- $n = 0.7$  Scaling factor

The cost of the reformer was determined in the same way, but the catalyst reformer has a replacement schedule of once a year.

$$C_{ref} = C_0 \cdot \left(\frac{S_1}{S_0}\right)^n$$

- $C_{ref}$  Reformer substitution cost
- $C_0 = 500 \text{ €}$  Reformer catalyst investment cost for  $S_0$  flow rate
- $S_1 = 380 \text{ m}^3/\text{h}$  Fuel flow rate
- $S_0 = 60 \text{ m}^3/\text{h}$  Reference flow rate
- $n = 1$  Scaling factor

Table 4.5 summarizes all costs considered and assumed for the natural gas fed SOFC configuration.

*Table 4.5 - Natural gas fed SOFC configuration costs breakdown*

| CAPEX                   |                    | OPEX                           |                    | INCOMES                |                    |
|-------------------------|--------------------|--------------------------------|--------------------|------------------------|--------------------|
| Plant preparation       | 200.000 €          | Natural gas                    | 1.879.050 €        | Biomethane injection   | 3.623.726 €        |
| SOFC                    | 4.800.000 €        | Reformer catalyst substitution | 3.167 €            | Electricity production | 1.089.853 €        |
| Thermal recovery system | 195.728 €          | Maintenance                    | 103.915 €          |                        |                    |
|                         |                    | Stack substitution             | 1.440.000 €        |                        |                    |
| <b>TOTAL</b>            | <b>5.195.728 €</b> | <b>TOTAL</b>                   | <b>1.986.131 €</b> | <b>TOTAL</b>           | <b>4.713.579 €</b> |

The annual electricity production, taking into account the continuous operation of the plant, is approximately 11.9 GWh. With a power consumption of around 8 GWh, the SOFC is also able to fully meet the power requirements of the entire plant, thus eliminating the cost of grid-supplied electricity. Based on the costs listed above, an economic analysis was carried out to identify the net present value (NPV) at 15 years, Figure 4.1, and the Payback time (PBT).

- $NPV_{5y} = 2.473.051 \text{ €}$



- NPV<sub>10y</sub> 9.111.078 €
- NPV<sub>15y</sub> 13.980.709 €
- PBT 5,4 years

$$\eta_g = \frac{W_{AC\ net} + Q_{HR}}{\dot{V}_{fuel} \cdot PCI_{NG}} = 0.59$$

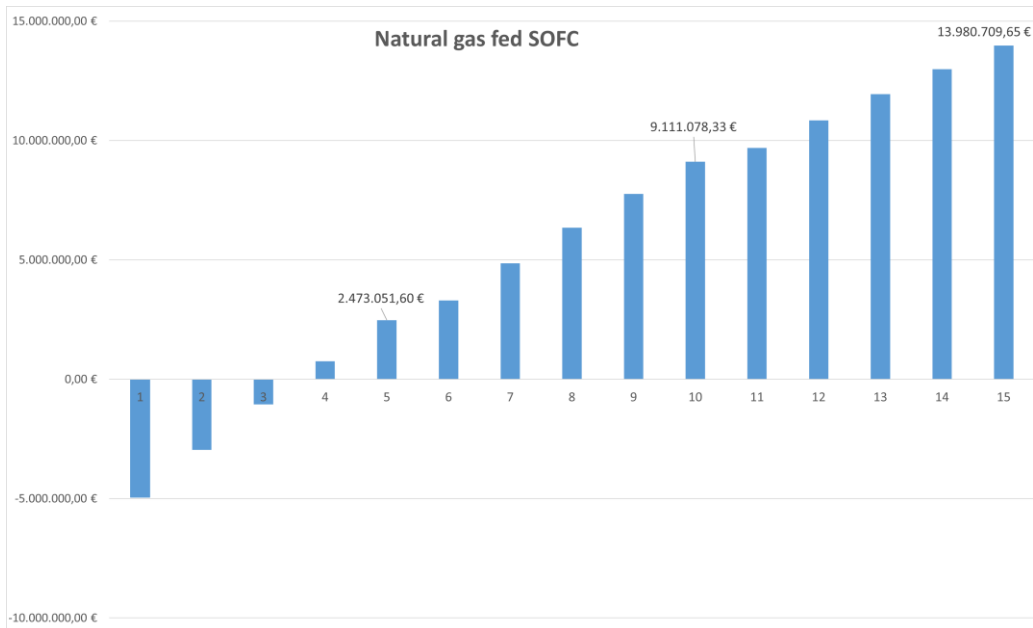


Figure 4.1 - Natural gas fed SOFC configuration NPV

Sensitivity analysis shows the trend of Payback time and Net Present Value over the range of unit costs for fuel cell purchases from 2 to 10 k€/kW. The results are shown in Figure 4.2 and 4.3, respectively.

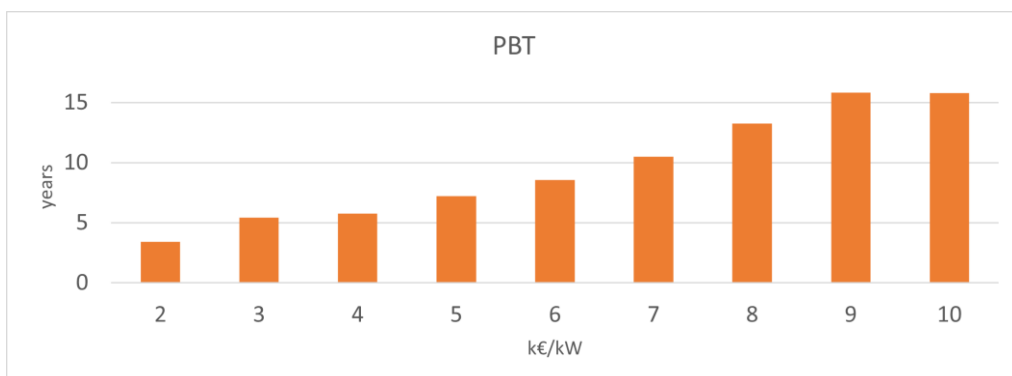


Figure 4.2 – Natural gas fed SOFC PBT Fuel cell unitary cost sensitivity analysis

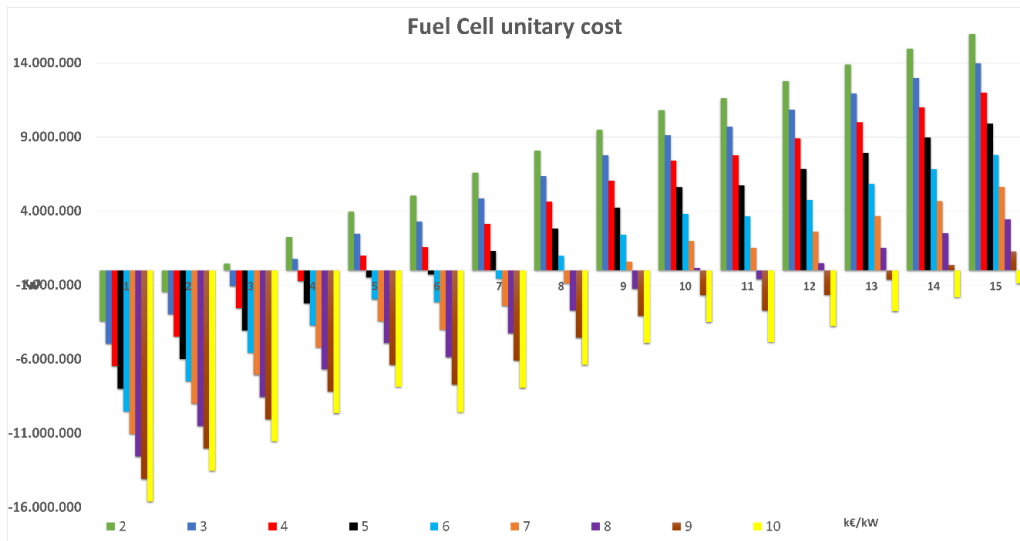


Figure 4.3 – Natural gas fed SOFC NPV fuel cell unitary cost sensitivity

### 4.3 Island SOFC configuration

The final configuration, modelled on Aspen, provides a fully self-sustaining operation and is therefore referred to as the “Island configuration”. In this configuration, the fuel cell stack is fuelled exclusively by biomethane produced by the digester rather than by natural gas taken from the grid. As the electricity needs are met by the production of the fuel cell, in this set-up, all energy withdrawals from the grid are thus set to zero. The share of biomethane for fuel cells was determined to be 39% of the annual biomethane production or about 2.340.000 Nm<sup>3</sup>. The hourly flow rate of biomethane will be approximately 270 m<sup>3</sup>/h. As in the case of the configuration fuelled by natural gas taken from the grid, the sizing criterion adopted for the stand-alone configuration was a quantity of thermal energy production sufficient to meet the needs of both the biodigester and the biocells. Table 4.6 shows the biomethane parameters for the Aspen simulation.

Table 4.6 – Biomethane parameters

|                                    |                       |
|------------------------------------|-----------------------|
| %CH <sub>4</sub> -%CO <sub>2</sub> | 60-40                 |
| Fuel density                       | 1,2 kg/m <sup>3</sup> |
| Fuel molecular weight              | 27,2 g/mol            |

From the model built on Aspen, the electrical output of this fuel cell stack was calculated to be 1.2 MWe. Since both the biomethane compressor, which is

needed to overcome the pressure drops generated within the fuel cell, and the cathode air fan are considered auxiliary utilities, their consumption must be deducted from the gross electrical power. The net AC power of the fuel cell stack is therefore approximately 1 MWe.

*Table 4.7 – Island SOFC configuration energy consumption and production*

|                            |             |
|----------------------------|-------------|
| $W_{\text{fuel blower}}$   | 2.043 W     |
| $W_{\text{air blower}}$    | 11.558 W    |
| $Q_{\text{Heat Recovery}}$ | 645.740 W   |
| $W_{\text{net AC}}$        | 1.055.272 W |

Four 250 kW modules were selected to accommodate commercially available electrical sizes. However, in the economic analysis, an additional 250 kW module was added (5x250 kW total) to cover periods of maintenance, either ordinary (stack replacement) or extraordinary, to still provide the power required to operate the municipal waste treatment plant, as it is a continuous operation. The cost analysis shown in the following graphs is based on a unit cost of 3 k€/kW. Although purchase costs for this type of technology are currently in the range of 2.5 to 3.5 k€/kW, a wider sensitivity analysis was also carried out in the range of 2 to 10 k€/kW (Figure 4.5 and Figure 4.6). Table 4.8 summarizes all costs considered and assumed for the natural gas fed SOFC configuration. In this configuration, the annual electricity production is approximately 9.2 GWh. As the estimated annual electricity consumption of the waste treatment plant is about 8 GWh, the demand is fully satisfied.

*Table 4.8 – Island SOFC configuration costs breakdown*

| CAPEX                   |                    | OPEX                           |                 | INCOMES                |                    |
|-------------------------|--------------------|--------------------------------|-----------------|------------------------|--------------------|
| Plant preparation       | 200.000 €          | Reformer catalyst substitution | 2.226 €         | Biomethane injection   | 2.210.473 €        |
| SOFC                    | 3.750.000 €        | Maintenance                    | 82.973 €        | Electricity production | 842.792 €          |
| Thermal recovery system | 198.628 €          | Stack substitution             | 1.125.000 €     |                        |                    |
| <b>TOTAL</b>            | <b>4.418.628 €</b> | <b>TOTAL</b>                   | <b>85.227 €</b> | <b>TOTAL</b>           | <b>3.053.265 €</b> |

Based on the costs listed above, an economic analysis was carried out to identify the net present value (NPV) at 15 years, Figure 4.4, and the Payback time (PBT).

- NPV<sub>5y</sub> 4.002.918 €
- NPV<sub>10y</sub> 11.354.609 €
- NPV<sub>15y</sub> 16.850.210 €
- PBT 4,2 years

$$\eta_g = \frac{W_{AC\ net} + Q_{HR}}{\dot{V}_{fuel} \cdot PCI_{NG}} = 0.64$$

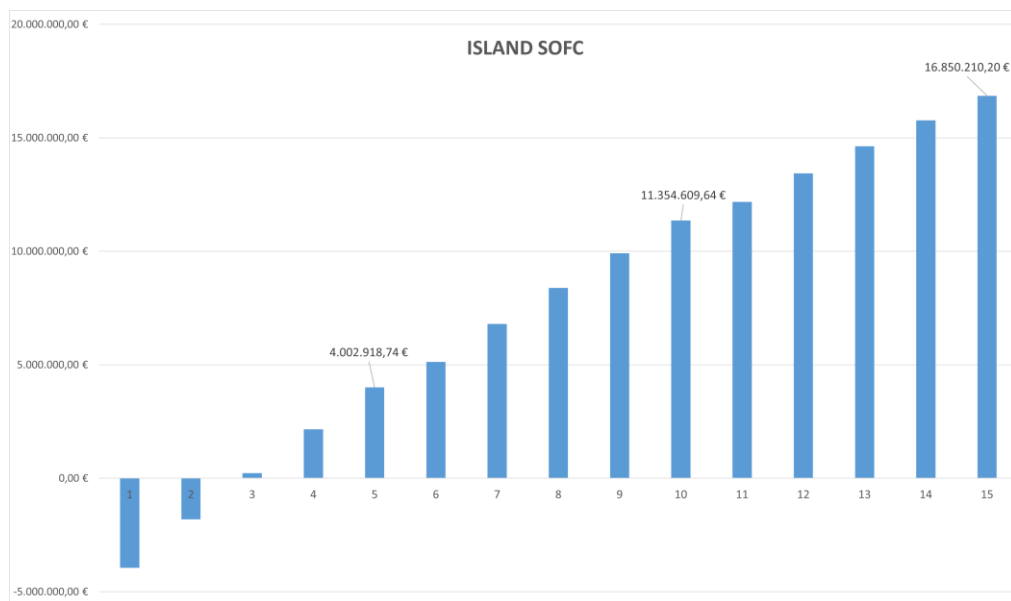


Figure 4.4 – Island SOFC configuration NPV

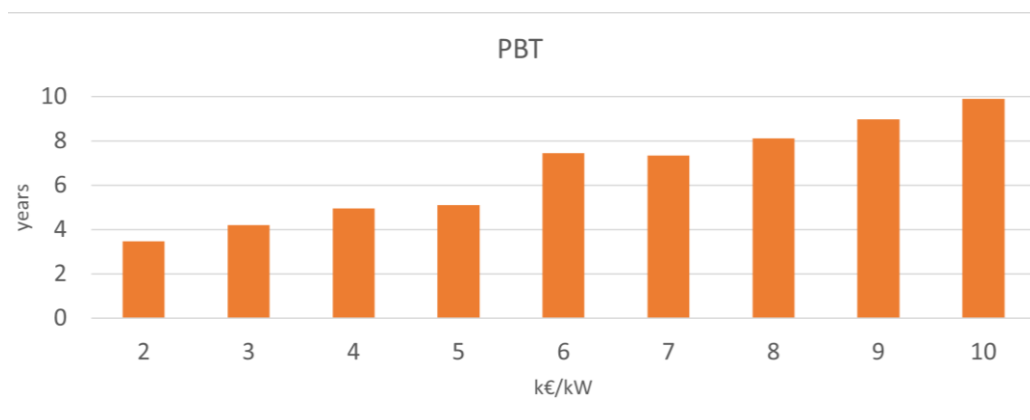


Figure 4.5 – Island SOFC PBT Fuel cell unitary cost sensitivity analysis

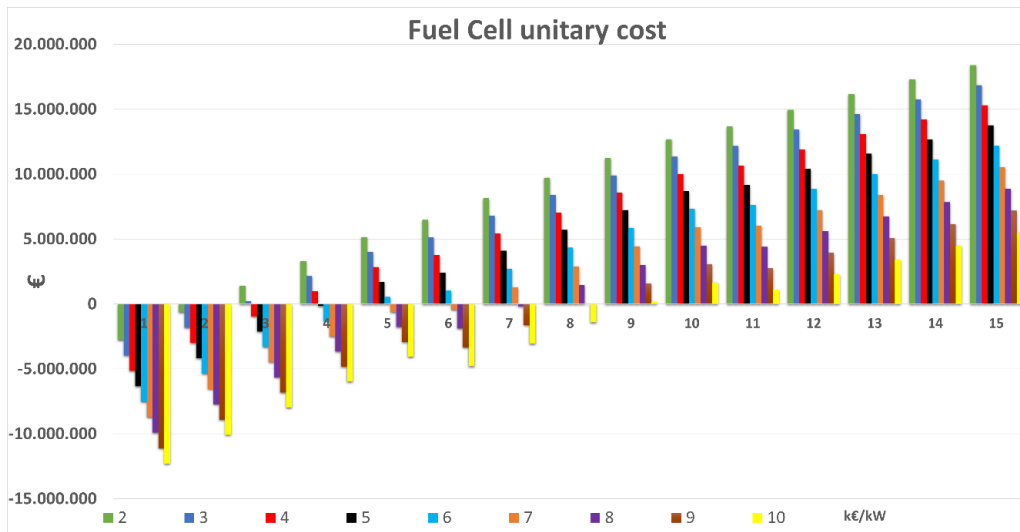


Figure 4.6 – Island SOFC NPV fuel cell unitary cost sensitivity

#### 4.4 Considerations

Given the possibility of choosing between two different configurations, it is appropriate to assess their criticalities and strengths by comparing them. In the natural gas-fuelled configuration, the same amount of thermal energy produced in the auxiliary heat exchanger (HX3), as well as that required to meet the thermal needs of the plant itself, requires a greater amount of gas than in the biomethane-fuelled configuration. This results in a higher hourly flow rate and therefore a higher power output. While this higher electrical output can be seen as an advantage, it must also be considered that it has a significant impact on the initial investment cost, as it depends on the installed electrical power. A further consideration is the cost of the fuel, in the first case natural gas taken from the distribution network and in the second case biomethane tapped before feeding into the network. Natural gas has to be purchased from the national distributor at market price and, given the quantities involved, will cost a not inconsiderable amount per year. On the other hand, the part of the biomethane "recirculated" to the fuel cell in the second configuration must be considered as a loss of revenue, since the national incentive is paid according to the amount of biomethane injected into the grid, which will therefore be lower. In addition, in the natural gas configuration, the annual fuel cost cannot be considered fixed, as it depends on the national price, which can fluctuate sharply in the event of certain events, as has happened recently due to pandemics and world conflicts. The difference in the island configuration is that the incentives are guaranteed for 15 years at the price agreed in the auction, so that the cost, or rather the

reduction in the remuneration for feeding biomethane into the grid due to the recirculation of the fuel to the fuel cell, can be considered a fixed amount and not dependent on fluctuations in the market price of gas. In both cases, the efficiency takes into account both electrical and thermal production, but as the hourly gas consumption is higher in the natural gas-fired configuration, while producing more electrical power, the overall efficiency will be higher in the island configuration as the hourly flow rate of biomethane is lower. Table 4.9 below summarises all the above comparisons.

*Table 4.9 – Configurations comparison*

|                                   | Base configuration | NG-fired SOFC | Island SOFC |
|-----------------------------------|--------------------|---------------|-------------|
| Electrical power [MWe]            | 0                  | 1.3           | 1           |
| Thermal power [kWt]               | 2x 780             | 632           | 645         |
| Global efficiency                 | 0.55               | 0.59          | 0.64        |
| Gas market price dependency       | YES                | YES           | NO          |
| Natural gas yearly cost [€]       | 406.428            | 1.879.050     | 0           |
| Electrical energy yearly cost [€] | 729.360            | 0             | 0           |

Another consideration in favour of the island configuration is CO<sub>2</sub> emissions to the atmosphere. As biomethane is produced from the anaerobic digestion of municipal solid waste and is therefore a renewable energy source, the CO<sub>2</sub> emissions are considered to be neutral or near-neutral in terms of carbon footprint. On the other hand, in the traditional configuration, combustion in natural gas boilers would result in the emission of approximately 1,455,372 tonnes of CO<sub>2</sub>e to the atmosphere per year. In conclusion, the choice of

configuration type is strongly influenced by the market price of natural gas, so that a hybrid configuration may be optimal: the basic configuration should be biomethane operation, as this is the most technically and economically efficient; in periods when the market price of natural gas is lower, one could opt to reduce the share of biomethane recycled at the expense of natural gas withdrawn from the grid. This would increase the revenues from the injection of biomethane into the grid, in line with the current incentives, while maintaining a good balance with the costs of purchasing natural gas from the grid.





## REFERENCES

- [1] IPCC, 2023: Climate Change 2023: Synthesis Report. Contribution of Working Groups I, II and III to the Sixth Assessment Report of the Intergovernmental Panel on Climate Change [Core Writing Team, H. Lee and J. Romero (eds.)]. IPCC, Geneva, Switzerland, pp. 35-115
- [2] H. Ritchie, M. Roser and P. Rosado (2020). "CO<sub>2</sub> and Greenhouse Gas Emissions". Published online at OurWorldInData.org. Retrieved from: <https://ourworldindata.org/co2-and-other-greenhouse-gas-emissions>
- [3] European Commission, Directorate-General for Climate Action, Going climate-neutral by 2050 – A strategic long-term vision for a prosperous, modern, competitive and climate-neutral EU economy, Publications Office, 2019, <https://data.europa.eu/doi/10.2834/02074>
- [4] K. Kordesch, G. K. Simader, Fuel Cells and their applications; Weinheim; New York; Basel; Cambridge; Tokyo: VHC, 1996.
- [5] J. Larminie, A. Dicks, Fuel Cell System Explained, Wiley, 2003.
- [6] Ruiz-Trejo, E. & Atkinson, Alan & Brandon, Nigel. (2015). Metallizing porous scaffolds as an alternative fabrication method for solid oxide fuel cell anodes. Journal of Power Sources. 280. 10.1016/j.jpowsour.2015.01.091.
- [7] Zhan, Yuedong & Zhu, Jianguo & Guo, Youguang & Wang, Hua. (2009). Performance analysis and evaluation of proton membrane exchange fuel cells. 2008 Australasian Universities Power Engineering Conference, AUPEC 2008. 1 - 6.

- [8] Syngas Production By Short Contact Time Catalytic Partial Oxidation of Methane - Scientific Figure on ResearchGate. Available from: [https://www.researchgate.net/figure/TEM-image-of-whiskers-carbon-on-Ni-MgAl-2-O-4-reforming-catalyst-readapted-from\\_fig5\\_235742050](https://www.researchgate.net/figure/TEM-image-of-whiskers-carbon-on-Ni-MgAl-2-O-4-reforming-catalyst-readapted-from_fig5_235742050) [accessed 18 Feb, 2024]
- [9] Rabuni, Mohamad Fairus, Tao Li, Mohd Hafiz Dzarfan Othman, Faidzul Hakim Adnan, and Kang Li. 2023. "Progress in Solid Oxide Fuel Cells with Hydrocarbon Fuels" *Energies* 16, no. 17: 6404. <https://doi.org/10.3390/en16176404>
- [10] Broering, Victor & Júnior, Orozimbo & Subtil de Oliveira, Nicolý & Ollhoff, Rüdiger & Almeida, Igor & Rosa, Edvaldo. (2023). Bioprocessing of broiler feathers to produce biomethane. *World's Poultry Science Journal*. 79. 1-20. [10.1080/00439339.2023.2175344](https://doi.org/10.1080/00439339.2023.2175344).
- [11] Adelaide Calbry-Muzyka, Hossein Madi, Florian Rüsç-Pfund, Marta Gandiglio, Serge Biollaz, Biogas composition from agricultural sources and organic fraction of municipal solid waste, *Renewable Energy*, Volume 181, 2022
- [12] Andrea Lanzini, Hossein Madi, Vitaliano Chiodo, Davide Papurello, Susanna Maisano, Massimo Santarelli, Jan Van herle, Dealing with fuel contaminants in biogas-fed solid oxide fuel cell (SOFC) and molten carbonate fuel cell (MCFC) plants: Degradation of catalytic and electro-catalytic active surfaces and related gas purification methods, *Progress in Energy and Combustion Science*, Volume 61, 2017

- [13] S. Ali Saadabadi, Aditya Thallam Thattai, Liyuan Fan, Ralph E.F. Lindeboom, Henri Spanjers, P.V. Aravind, Solid Oxide Fuel Cells fuelled with biogas: Potential and constraints, *Renewable Energy*, Volume 134, 2019
- [14] Cimenti M, Hill JM. Direct Utilization of Liquid Fuels in SOFC for Portable Applications: Challenges for the Selection of Alternative Anodes. *Energies*. 2009; 2(2):377-410 <http://doi.org/10.3390/en20200377>
- [15] B. Tjaden, M. Gandiglio, A. Lanzini, M. Santarelli, and M.Järvinen – Small-scale Biogas-SOFC Plant: Technical Analysis and Assessment of Different Fuel Reforming Option *Energy & Fuel* 2014 16
- [16] SFRP-RTY-000002-BGAS Rev. n.0, Centrale di San Filippo – Impianto di trattamento e recupero della FORSU – Relazione Tecnica